

# Journal Pre-proof

Evoking highly focal percepts in the fingertips through targeted stimulation of sulcal regions of the brain for sensory restoration

Santosh Chandrasekaran, Stephan Bickel, Jose L. Herrero, Joo-won Kim, Noah Markowitz, Elizabeth Espinal, Nikunj A. Bhagat, Richard Ramdeo, Junqian Xu, Matthew F. Glasser, Chad E. Bouton, Ashesh D. Mehta

PII: S1935-861X(21)00147-9

DOI: <https://doi.org/10.1016/j.brs.2021.07.009>

Reference: BRS 2007

To appear in: *Brain Stimulation*

Received Date: 2 February 2021

Revised Date: 29 June 2021

Accepted Date: 19 July 2021

Please cite this article as: Chandrasekaran S, Bickel S, Herrero JL, Kim J-w, Markowitz N, Espinal E, Bhagat NA, Ramdeo R, Xu J, Glasser MF, Bouton CE, Mehta AD, Evoking highly focal percepts in the fingertips through targeted stimulation of sulcal regions of the brain for sensory restoration, *Brain Stimulation* (2021), doi: <https://doi.org/10.1016/j.brs.2021.07.009>.

This is a PDF file of an article that has undergone enhancements after acceptance, such as the addition of a cover page and metadata, and formatting for readability, but it is not yet the definitive version of record. This version will undergo additional copyediting, typesetting and review before it is published in its final form, but we are providing this version to give early visibility of the article. Please note that, during the production process, errors may be discovered which could affect the content, and all legal disclaimers that apply to the journal pertain.

© 2021 Published by Elsevier Inc.

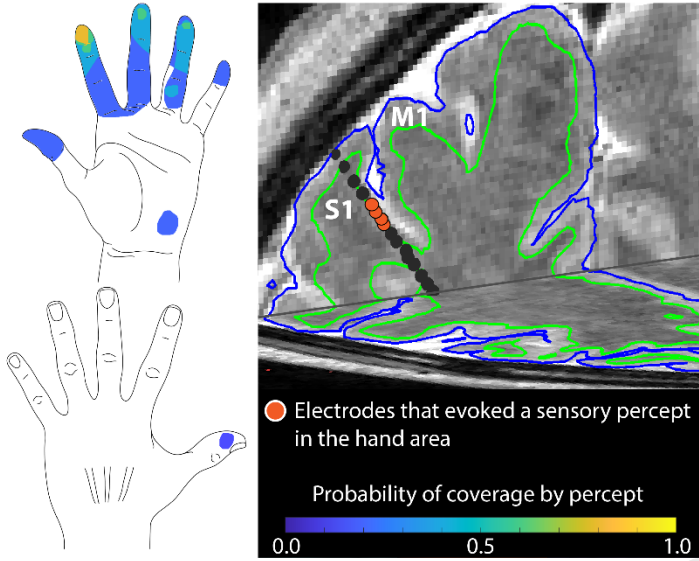


**Author Contributions**

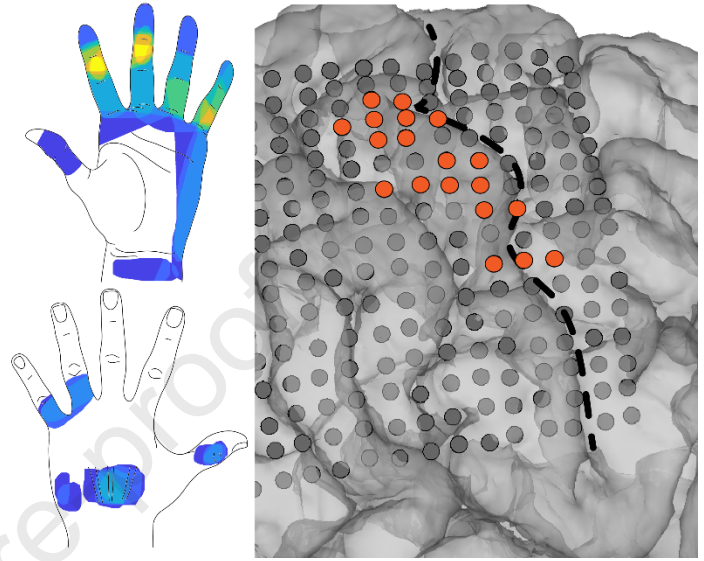
SB, JLH, CEB and ADM designed the study. JWK and JX designed and performed the fMRI procedures at Icahn School of Medicine at Mount Sinai and analyzed the data. ADM performed the SEEG leads and HD-ECOG grid implantations. NM and EE digitized and co-registered the electrode locations. SC, SB, NAB, RR and CEB performed all the experiments. SC and CEB analyzed data from these experiments. MFG and JX provided key insights into cortical anatomy, help using the workbench software and generating relevant figures for the manuscript. All authors contributed towards interpreting the results of the experiments. SC and CEB finished the initial draft of the paper and all authors provided critical review, edits and approval of the final manuscript.

## Graphical Abstract

## SEEG-mediated sulcal stimulation of S1



## HD-ECoG mediated gyral stimulation of S1



1 **Evoking highly focal percepts in the fingertips through targeted stimulation of**  
2 **sulcal regions of the brain for sensory restoration**

3 Santosh Chandrasekaran<sup>1\*</sup>, Stephan Bickel<sup>2,3,4\*</sup>, Jose L Herrero<sup>2,3</sup>, Joo-won Kim<sup>5</sup>, Noah  
4 Markowitz<sup>2</sup>, Elizabeth Espinal<sup>2</sup>, Nikunj A Bhagat<sup>1</sup>, Richard Ramdeo<sup>1</sup>, Junqian Xu<sup>5</sup>, Matthew F  
5 Glasser<sup>6</sup>, Chad E Bouton<sup>1,7†</sup> and Ashesh D Mehta<sup>2,3†</sup>

6 <sup>1</sup>Neural Bypass and Brain Computer Interface Laboratory, Feinstein Institutes for Medical Research,  
7 Northwell Health, Manhasset, NY

8 <sup>2</sup>The Human Brain Mapping Laboratory, Feinstein Institutes for Medical Research, Northwell Health,  
9 Manhasset, NY

10 <sup>3</sup>Department of Neurosurgery and <sup>4</sup>Neurology, Donald and Barbara Zucker School of Medicine at  
11 Hofstra/Northwell, Manhasset, NY

12 <sup>5</sup>Departments of Radiology and Psychiatry, Baylor College of Medicine, Houston, TX

13 <sup>6</sup>Departments of Radiology and Neuroscience, Washington University in St Louis, Saint Louis, MO

14 <sup>7</sup>Department of Molecular Medicine, Donald and Barbara Zucker School of Medicine at  
15 Hofstra/Northwell, Manhasset, NY

16 \*These authors contributed equally to this work.

17 †These authors share senior authorship.

18 **Corresponding authors:** Santosh Chandrasekaran and Chad E Bouton

19 **Email:** [schandraseka@northwell.edu](mailto:schandraseka@northwell.edu), [cbouton@northwell.edu](mailto:cbouton@northwell.edu)

20 **Author Contributions**

21 SB, JLH, CEB and ADM designed the study. JWK and JX designed and performed the fMRI  
22 procedures at Icahn School of Medicine at Mount Sinai and analyzed the data. ADM performed  
23 the SEEG leads and HD-ECOG grid implantations. NM and EE digitized and co-registered the  
24 electrode locations. SC, SB, NAB, RR and CEB performed all the experiments. SC and CEB  
25 analyzed data from these experiments. MFG and JX provided key insights into cortical anatomy,  
26 help using the workbench software and generating relevant figures for the manuscript. All  
27 authors contributed towards interpreting the results of the experiments. SC and CEB finished the  
28 initial draft of the paper and all authors provided critical review, edits and approval of the final  
29 manuscript.

### 30 **Competing Interest Statement**

31 The authors have no conflicting financial interests.

32 **Keywords:** Fingertip representation, Sensory percepts, Sensory restoration,

33 Stereoelectroencephalography depth electrodes, Brain-computer interface.

### 34 **This PDF file includes:**

35 Main Text

36 Figures 1 to 5

37 Supplementary Figure 1 to 1

### 38 **Abstract**

39 **Background:** Paralysis and neuropathy, affecting millions of people worldwide, can be  
40 accompanied by significant loss of somatosensation. With tactile sensation being central to  
41 achieving dexterous movement, brain-computer interface (BCI) researchers have used  
42 intracortical and cortical surface electrical stimulation to restore somatotopically-relevant  
43 sensation to the hand. However, these approaches are restricted to stimulating the gyral areas of  
44 the brain. Since representation of distal regions of the hand extends into the sulcal regions of  
45 human primary somatosensory cortex (S1), it has been challenging to evoke sensory percepts  
46 localized to the fingertips.

47 **Objective/Hypothesis:** Targeted stimulation of sulcal regions of S1, using  
48 stereoelectroencephalography (SEEG) depth electrodes, can evoke focal sensory percepts in the  
49 fingertips.

50 **Methods:** Two participants with intractable epilepsy received cortical stimulation both at the  
51 gyri via high-density electrocorticography (HD-ECOG) grids and in the sulci via SEEG depth  
52 electrode leads. We characterized the evoked sensory percepts localized to the hand.

53 **Results:** We show that highly focal percepts can be evoked in the fingertips of the hand through  
54 sulcal stimulation. fMRI, myelin content, and cortical thickness maps from the Human  
55 Connectome Project elucidated specific cortical areas and sub-regions within S1 that evoked  
56 these focal percepts. Within-participant comparisons showed that percepts evoked by sulcal  
57 stimulation via SEEG electrodes were significantly more focal (80% less area;  $p=0.02$ ) and

58 localized to the fingertips more often, than by gyral stimulation via HD-ECOG electrodes.  
59 Finally, sulcal locations with consistent modulation of high-frequency neural activity during  
60 mechanical tactile stimulation of the fingertips showed the same somatotopic correspondence as  
61 cortical stimulation.

62 **Conclusions:** Our findings indicate minimally invasive sulcal stimulation via SEEG electrodes  
63 could be a clinically viable approach to restoring sensation.

#### 64 **Highlights**

- 65 • Stimulation of S1 sulcal regions via minimally invasive stereoelectroencephalography  
66 (SEEG) electrodes localized evoked percepts to fingertips more often than gyral  
67 stimulation.
- 68 • fMRI, myelin, and cortical thickness maps from Human Connectome Project delineated  
69 hand and finger representation in sulcal S1.
- 70 • Sulcal stimulation evoked percepts that were more focal than those evoked by cortical  
71 surface stimulation at the postcentral gyrus.
- 72 • Neural activity recorded in sulcal areas strongly correlated to mechanical tactile  
73 stimulation.

#### 74 **Introduction**

75 Over 5 million people are living with paralysis in the United States alone [1] with spinal  
76 cord injury (SCI) being one of the leading causes. Up to 12% of individuals with SCI have  
77 complete tetraplegia and experience total loss of upper limb somatosensation [2]. Meanwhile, of  
78 422 million people worldwide with diabetes mellitus [3], up to 64% can experience peripheral  
79 neuropathy leading to significant impairment of the sense of touch [4]. Such loss of sensation  
80 critically impairs the ability to perform dexterous manipulation of objects [5,6]. Intracortical brain-  
81 computer interfaces (BCI) have shown tremendous success in decoding intended movements from  
82 neural activity recorded in the primary motor cortex [7,8] and subsequently, restoring motor  
83 control of their own hand in people with tetraplegia [9]. However, this significant progress in  
84 neurorehabilitation is often hampered by the lack of tactile feedback. Without somatosensation,

85 users of BCI systems rely heavily on visual feedback while interacting with objects precluding  
86 fine motor control, such as manipulation of small objects, inability to detect object contact to  
87 transition from reaching to grasping, modifying grasp strength to prevent slipping, or interacting  
88 with objects outside the line of sight.

89         Recently, tactile percepts in the hand have been evoked in humans through intracortical  
90 microstimulation using microelectrode arrays [10–12] or cortical surface stimulation using  
91 electrocorticography (ECoG) grids [13–15] in the primary somatosensory cortex (S1), specifically  
92 cortical area 1. Although such artificial sensory feedback helps improve the user performance with  
93 a BCI system [16], focal percepts in fingertips that would be critical for dexterous manipulations  
94 as those mentioned above [17] have been difficult to achieve. In a recent study, targeting fingertip  
95 representations in the cortex required extensive intraoperative mapping using mechanical  
96 stimulation at the periphery [12] relying on spared neural pathways which may not be feasible in  
97 many patients with SCI. A primary reason for the inability to reliably evoke fingertip percepts  
98 could be that cortical stimulation in these studies has been restricted to the gyral areas of S1, i.e.,  
99 the postcentral gyrus, or area 1.

100         Functional magnetic resonance imaging (fMRI) has shown individual digit representations  
101 to occur in the central and postcentral sulcus in addition to the postcentral gyrus, covering the  
102 cytoarchitectonically distinct cortical areas 3a, 3b, 1 and 2 [18–21]. As observed in non-human  
103 primates [22–24], these imaging studies suggest that a mirror-reversal of phalange representation  
104 occurs at the area 3b/1 border located in the central sulcus close to the crown of the postcentral  
105 gyrus. This places the proximal phalanges close to that border while more distal phalanges,  
106 including the fingertips, occur towards the area 3a/3b border located on the posterior wall of the  
107 central sulcus [18,25]. Another representation of the distal phalanges appears to occur in area 1,  
108 towards the posterior regions of the postcentral gyrus [18,25,26]. This would be consistent with  
109 the observations from a recent human somatosensory mapping study [27]. However, other studies  
110 show representation of distal phalanges closer to the 3b/1 border [28,29]. Thus, it is still unclear  
111 how the fingertip representation is distributed across the central sulcus and postcentral gyrus in  
112 human S1 [30].

113         Recent advances in stereotactic placement of depth electrodes, also known as  
114 stereoelectroencephalography (SEEG), increasingly provide reliable access to deeper cortical and

115 subcortical targets in the brain [31]. These electrodes are increasingly used in the clinic for seizure  
116 onset localization in patients with medically refractory epilepsy [32]. In addition, SEEG electrodes  
117 have been used to map and document the sensory percepts evoked while stimulating the human  
118 parietal [33] and insular cortices [34]. Comparing separate cases involving SEEG and ECoG  
119 implantations, SEEG electrodes have been shown to be a clinically useful alternative for electrical  
120 brain stimulation (EBS) to map eloquent cortical areas [35,36]. In fact, a recent study showed that  
121 SEEG-mediated EBS could identify sensorimotor areas with high accuracy and specificity [37].  
122 Moreover, implantation procedures for SEEG electrodes are minimally invasive (~2mm  
123 craniostomy) with lower rates of infection [38] compared to subdural strip and ECoG electrodes  
124 which require a craniotomy several centimeters wide [39].

125         In this first-in-human study, we explored the representation of the hand in the sulcal regions  
126 of S1 using SEEG electrodes. We implanted both SEEG and HD-ECoG electrodes in the sulcal  
127 and gyral areas of S1, respectively, in two patients with intractable epilepsy. A within-participant  
128 comparison of the percepts evoked by the two electrode types allowed us to map the hand  
129 representations in both the gyral and sulcal areas of S1 and compare the corresponding evoked  
130 percepts. Electrode implantation was guided by high-resolution fMRI obtained during a finger-  
131 tapping task analyzed using the processing pipelines of the Human Connectome Project (HCP).  
132 Upon administering intracortical direct electrical stimulation to the sulcal or gyral areas, the  
133 participants reported sensory percepts that were localized to the contralateral arm, hand, and even  
134 fingertips. Strikingly, we observed that tactile percepts evoked by sulcal stimulation were much  
135 more focused in their spatial extent. Furthermore, the percepts evoked by sulcal stimulation tended  
136 to be in and around the fingertips more often. T1-weighted (T1w) and T2-weighted (T2w)  
137 structural images provided the T1w/T2w-based myelin content and cortical thickness maps which  
138 enabled atlas-based parcellation of the cortical areas, somatotopic subregions, and sub-areas of the  
139 sensorimotor cortex [40] further informing location of electrodes and the corresponding evoked  
140 percepts. SEEG-mediated recording of neural activity in the sulcal areas evoked upon mechanical  
141 tactile stimulation enabled precise localization of cortical regions involved in processing of  
142 sensory information from specific finger and palm regions.

143         These results demonstrate that stimulation of sulcal regions of S1 can be achieved using  
144 SEEG and can activate fingertip representations. Combined with the minimally invasive

145 implantation procedure for SEEG electrodes, this approach for sulcal stimulation can be an  
146 effective and reliable for evoking focal percepts in the hand and fingers that are functionally  
147 relevant to people with tetraplegia. Furthermore, they can be an effective tool for passive mapping  
148 of the brain for clinical purposes.

## 149 **Methods**

150 *Participants:* Two patients undergoing pre-operative seizure monitoring for surgical treatment of  
151 intractable epilepsy took part in this study. Participant 1 was implanted with SEEG leads for 7  
152 days after which they were explanted. Mapping of percepts evoked by stimulating through these  
153 electrodes was performed on Day 6 post-implant. About 3 months later, the patient was  
154 implanted with HD-ECOG grids for 8 days and percept mapping was performed on day 7 post-  
155 implant. In case of participant 2, SEEG leads were implanted for 14 days. About a month later,  
156 the participant was implanted with HD-ECOG grids for 10 days. Recording of neural activity  
157 with SEEG electrodes in response to peripheral tactile stimulation was done on Day 9 post-  
158 implant. Percept mapping was performed on Day 12 and Day 9 for SEEG and HD-ECOG  
159 electrodes, respectively. Recording of neural activity using SEEG electrodes helped localize the  
160 seizure onset close to the sensorimotor areas. However, additional grid electrodes were needed to  
161 further localize the seizure onset and, more importantly, the borders of sensorimotor cortices to  
162 help guide the resection. This two-staged approach of implanting SEEG leads followed by grid  
163 and/or strip electrodes is often used in such a situation at the Comprehensive Epilepsy Center at  
164 Northwell Health.

165 The decisions regarding whether to implant, the electrode targets, and the duration for  
166 implantation were based entirely on clinical grounds without reference to this investigation.  
167 Based on these clinical indications, all electrodes were implanted in the right hemisphere for  
168 both participants. Patients were informed that participation in this study would not alter their  
169 clinical treatment, and that they could withdraw from the study at any time without jeopardizing  
170 their clinical care. All procedures and experiments were approved by the Northwell Institutional  
171 Review Board and participants provided informed consent prior to enrollment into the study.

172 *Imaging:* Participants were scanned a week before their first implant on a 3T MRI scanner  
173 (Skyra, Siemens, Germany) with a 32-channel head coil. HCP-like structural and functional MRI  
174 were acquired: T1-weighted (T1w) 3D MPRAGE sequence, 0.8 mm isotropic resolution,

175 TR/TE/TI = 2400/2.07/1000 ms, flip angle = 8 degree, in-plane under-sampling (GRAPPA) = 2,  
176 acquisition time 7 min; T2-weighted (T2w) 3D turbo spin echo (SPACE) sequence, 0.8 mm  
177 isotropic resolution, in-plane under-sampling (GRAPPA) = 2, TR/TE = 3200/564 ms, acquisition  
178 time 6.75 min; task fMRI using the CMRR implementation of multiband gradient echo echo-  
179 planar imaging (EPI) sequence [41], 2.1 mm isotropic resolution, 70 slices with a multiband  
180 factor of 7 [42], FOV 228 mm × 228 mm, matrix size 108 × 108, phase partial Fourier 7/8,  
181 TR/TE = 1000/35 ms, flip angle = 60 degree, phase encoding direction = anterior-posterior (A-  
182 P), echo spacing = 0.68 ms, 240 volumes in 4 min; and a pair of reversed polarity (A-P / P-A)  
183 spin echo EPI field mapping acquisitions with matched echo train length and echo spacing to the  
184 fMRI acquisition. The task was button-pressing on the PST button response unit (Psychology  
185 Software Tools, Sharpsburg, PA, USA) using a single finger (wrist restrained with strap on the  
186 button response unit and neighboring fingers taped down with medical tape), repeating 6 times of  
187 20-second off (resting with cue of a blank dark screen) and 20-second on (tapping with  
188 continuous video cue of the same finger motion presented from a projector screen). Participant 1  
189 performed task once for each of thumb, index, and little fingers (phase-encoding direction A->P)  
190 while participant 2 performed two repetitions for each of thumb, index, and middle fingers  
191 (phase-encoding directions A->P and P->A). Due to limited scanner time, we consistently used  
192 three fingers in the button task. The motivation for including digits 1, 2, and 5 in participant 1  
193 was to map the extents of the hand while in participant 2, our motivation evolved to focus on the  
194 first three digits as they are functionally more important in grasping and manipulating objects.  
195 The MRI preprocessing began with the HCP minimal preprocessing pipelines version 3.27 [43]  
196 including, motion correction, distortion correction, cortical surface reconstruction and subcortical  
197 segmentation, generation of T1w/T2w-based myelin content and cortical thickness maps,  
198 transformation of the fMRI data to MNI and CIFTI grayordinate standard spaces using folding-  
199 based registration with MSMSulc [44,45], and 2 mm FWHM surface and subcortical parcel  
200 constrained smoothing for regularization. The fMRI data were cleaned of spatially specific  
201 structured noise using the HCP's multi-run (version 4.0) ICA-FIX [46–48] for multi fMRI  
202 (multiple finger tasks) and linear trends without regressing out motion parameters. Somatotopic  
203 functional responses were estimated (first-level for participant 1 and second-level fixed-effect  
204 averaging of the two phase-encoding directions for participant 2) using a generalized linear  
205 model (GLM)-based fMRI analysis [49] on the grayordinate data space for each finger.

206 *Electrode localization:* The SEEG electrodes (Model Number 2102-16-093, PMT Corporation,  
 207 Chanhassen, MN, USA) consisted of 16 contacts, cylinders with 2 mm length, 0.8 mm diameter,  
 208 and 4.43 mm spacing (center to center) with about 5.02 mm<sup>2</sup> of surface area per contact. The  
 209 lead spanned a length of 68.5 mm from tip to end of last contact. The HD-ECOG grids (PMT  
 210 Corporation) consisted of 2 mm diameter flat contacts with 3.14 mm<sup>2</sup> surface area per contact, in  
 211 an 8x8 arrangement with 5 mm spacing (center to center) in participant 1 with and a 16x16  
 212 contact arrangement with 4 mm spacing in participant 2. Since both patients had clinical  
 213 indications that required mapping of the sensorimotor cortex, task-based fMRI activation maps  
 214 were used to guide electrode placement.

215 For digital localization of the electrodes, we used the freely available iElvis toolbox,  
 216 available at <https://github.com/iELVis/> [50]. Briefly, the electrodes were manually localized  
 217 using the software BioImage Suite (<http://www.bioimagesuite.org>) on a postimplant CT which  
 218 was co-registered using an affine transformation (6 degrees-of-freedom FLIRT;  
 219 [www.fmrib.ox.ac.uk/fsl](http://www.fmrib.ox.ac.uk/fsl)) to a pre-implantation 3T high-resolution T1w MRI. We used the  
 220 FreeSurfer [51] output from the HCP minimal processing pipeline [40] to obtain the pial surface.  
 221 The subdural HD-ECOG electrodes were projected to the smoothed pial surface. The smoothed  
 222 pial surface, also called the outer smoothed surface, is generated by Freesurfer and wraps tightly  
 223 around the gyral surfaces of the pial layer while bridging over the sulci. No correction was  
 224 applied to SEEG electrode coordinates.

225 To visualize the fMRI activation maps and the electrodes simultaneously, we used HCP  
 226 Connectome Workbench. Before importing the electrode coordinates into Workbench, we  
 227 applied a RAS coordinate offset (the right-hand coordinate system of R = thumb, A = index, and  
 228 S = middle finger) as follows –

$$229 \quad \textit{transformed\_RAS\_coordinates} = \textit{Norig} * \textit{inv}(\textit{Torig}) * \textit{RAS\_coordinates}$$

230 where the transformation matrices *Norig* is obtained by *mri\_info --vox2ras*

231 *[subject]/mri/orig.mgz* and *Torig* is obtained by *mri\_info --vox2ras-tnr [subject]/mri/orig.mgz*

232 The transformed coordinates were then imported as foci using the T1w surfaces into a  
 233 developmental version of Connectome Workbench.

234 *Electrical brain stimulation (EBS)*: Intracranial EBS is a routine clinical procedure to identify  
235 eloquent cortex to be spared from surgical resection. Generally, EBS was carried out towards the  
236 end of implantation period after sufficient seizure data had been collected and participants were  
237 back on their anti-seizure medications.

238 For this study, we used routine EBS parameters with a S12D Grass current-controlled  
239 cortical stimulator (Grass Technologies, Pleasanton, CA). We used pairs of electrodes for bipolar  
240 stimulation and delivered current-regulated, symmetric biphasic square-wave pulses with 0.2 ms  
241 width per phase, at 20 or 50 Hz, with stimulation amplitudes between 0.5–6 mA, for 0.5–2  
242 seconds while the participant was quietly resting and asked to report the occurrence of any  
243 sensation. The different sites were first screened for a possible percept with 50 Hz stimulation –  
244 a stimulation frequency that provides a good trade-off between obtaining a stimulation effect and  
245 eliciting a seizure and is in accordance with common procedure established across up to 70% of  
246 epilepsy monitoring centers [52]. The stimulation amplitude was initially set at 0.5 mA – the  
247 lowest possible amplitude on the clinical stimulator. If no percept was evoked, the stimulation  
248 amplitude was increased in gross (~0.5mA) increments until a percept was elicited, or after-  
249 discharges occurred, up to a maximal amplitude of 6 mA. Once a percept was felt the amplitude  
250 was more finely adjusted (using the analogue adjustment knob) to find the threshold of  
251 perception. The stimulation was repeated at this final threshold value at least two times to ensure  
252 the evoked percept was consistent. If a percept was evoked even at 0.5 mA at 50 Hz, the  
253 frequency was decreased to the next frequency (20 Hz) and the above process was repeated. The  
254 stimulation pulse had a cathodic leading phase. Stimulation time was always limited to a  
255 maximum of 2 seconds. Stimulation was stopped immediately and much before the maximum  
256 time had elapsed if the subject reported a sensation. For every sensation on the hand that was  
257 reported, the participant was asked to draw the affected area on a schematic of a hand. The  
258 sensations were described as “tingling” or “sensation of electricity”. While the intensity of the  
259 percepts changed with stimulation amplitude, none of the other qualities of the evoked percepts  
260 such as location, size, and qualitative description changed with stimulation amplitude.

261 Without informing the participant, sham trials (0 mA stimulation) were intermixed with  
262 real stimulation trials to rule out any placebo effects. Intracranial EEG was acquired  
263 continuously using a clinical recording system (XLTEK, Natus Medical) at 512 Hz or 1 kHz and

264 monitored across all implanted electrodes for the presence of after-discharges and seizures. No  
265 seizures were caused during stimulation of the areas reported here.

266 *Analysis of sensory percepts:* For this study, we focused our analysis to the sensory percepts  
267 localized to the hand and wrist. Some of the SEEG and HD-ECOG electrodes did evoke complex  
268 percepts that included both sensory as well as motor components, including percepts that were  
269 accompanied with an overt movement or a sensation of movement, presumably a proprioceptive  
270 sensation. We included only those electrodes that evoked a tactile sensation by itself, without any  
271 overt or perceived sensation of movement. To digitize the participant responses, we used a script  
272 custom-written in MATLAB to redraw the participant drawings on a computer. Surface areas of  
273 the digitized percepts were then calculated and used for all further analysis.

274 *Recording of neural activity:* In addition to the clinical recording system, neural activity was  
275 recorded for participant 2 using SEEG electrodes with a Neuroport System (Blackrock  
276 Microsystems, Salt Lake, Utah) with a sampling rate of 10 kHz while performing mechanical  
277 stimulation of the fingertips of their left hand. We used a Semmes-Weinstein Monofilament  
278 (TouchTest Sensory Probes) of evaluator size, 4.31 (2 g). A visual cue, visible only to the  
279 experimenter and not the participant, signaled the start and end of each repetition as well as the  
280 specific finger to which the mechanical stimuli was to be targeted. During this period, the  
281 experimenter repeatedly tapped the cued finger with a Semmes-Weinstein Monofilament  
282 repeatedly, approximately once every second. This cue signal was aligned to the recorded neural  
283 data to analyze only the epochs of stimuli. Due to time constraints and patient fatigue, we  
284 unfortunately were not able to perform the recording task in participant 1.

285 Two separate electrodes located in soft tissue lacking neural activity were used for the  
286 system ground and for the reference. Subsequent analysis involved multiple steps to extract  
287 information regarding power modulation in different frequency bands. Signals from neighboring  
288 electrodes were subtracted in software to provide bipolar data with reduced noise. Non-  
289 overlapping Blackman windows of 200 ms in length were applied, followed by a short Fast Fourier  
290 Transform (sFFT) for each window (with a resulting frequency resolution of 5 Hz). The signal  
291 amplitudes at each frequency were then integrated (averaged) across pre-selected frequency bands  
292 as follows: 0–10, 10–15, 15–30, 30–100, 100–500, and 500–5000 Hz. These frequency bands have  
293 been shown to contain signals with amplitude modulation with a high degree of repeatability (high

294 temporal correlation) related to movement and tactile stimuli [53]. These amplitude features for  
295 all bipolar recordings were standardized by subtracting their mean and dividing by their standard  
296 deviation across the entire task. For the analysis in this study, we chose neural activity in the high  
297 gamma or 100-500 Hz frequency band. Numerous invasive studies have shown that high-gamma  
298 power changes in the sensorimotor area are associated with passive somatosensory stimulation  
299 [54–56]. Epochs aligned with each visual cue (animated hand) presented to the participant during  
300 each task were created, starting at the cue onset, and extending to 400 ms after the cue offset. All  
301 aligned trials for each epoch (cue) type were averaged to form a composite temporal response. To  
302 quantify the degree of repeatability, or temporal correlation, the mean correlation coefficient  
303 (MCC) was computed by averaging the correlation coefficients obtained for the amplitude features  
304 for each trial with respect to their cue-aligned composite [53].

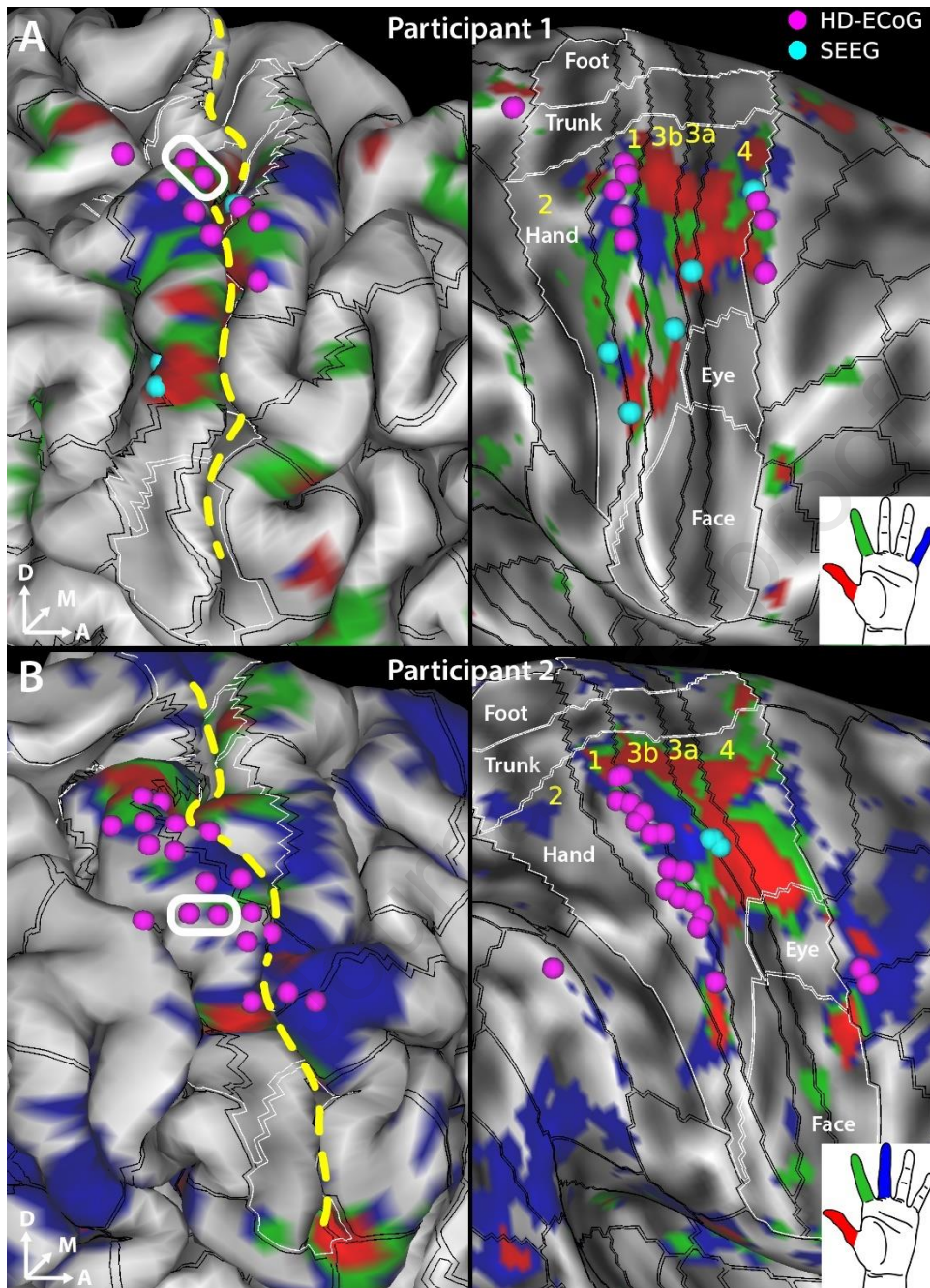
## 305 **Results**

306 Study participants were first implanted with SEEG leads, subsequently replaced by a HD-  
307 ECoG grid, for extraoperative monitoring of neural activity to localize the epileptogenic zone.  
308 During routine clinical intracranial EBS using either of these electrodes, participants were asked  
309 to report the sensory percepts that were evoked. A total of 28 SEEG electrode contacts each were  
310 localized to S1 and the nearby white matter in the two participants. For HD-ECoG, participant 1  
311 had 22 contacts over S1 while participant 2 had 57 contacts over S1 (

312 Table *I*). For this study, we focused on the sensory percepts localized to the hand and  
313 wrist. Stimulation amplitudes that evoked sensations in the hand area ranged from 0.5–6 mA  
314 with stimulation frequencies of either 20 or 50 Hz, and a pulse width of 200  $\mu$ s. After each  
315 stimulation trial (lasting 0.5–2 s), the evoked percept was reported by the participant and was  
316 recorded by the experimenter. A total of 40 electrode pairs (5 & 6 SEEG electrode pairs, and 10  
317 & 19 HD-ECoG electrode pairs in participants 1 and 2, respectively) across the two participants  
318 evoked at least one sensory percept in the contralateral hand or arm. Other electrodes evoked  
319 percepts that were localized to more proximal areas of the arm or even perceived bilaterally.  
320 These were not included for analysis in this study. The mean stimulus amplitude for SEEG-  
321 mediated sulcal stimulation at threshold of perception was  $1.09 \pm 1.07$  mA and  $1.59 \pm 1.68$  mA  
322 for participants 1 and 2, respectively given stimulation frequency of predominantly 20 Hz.  
323 Meanwhile, mean stimulus amplitude at threshold for gyral stimulation with HD-ECoG  
324 electrodes was  $0.989 \pm 0.37$  mA and  $2.25 \pm 1.23$  mA for participants 1 and 2, respectively with a  
325 stimulation frequency of 50 Hz. It is worth noting that the stimulation frequency had to be  
326 lowered to 20 Hz to determine the thresholds for SEEG electrodes as compared to HD-ECoG  
327 electrodes (50 Hz). Since the lowest stimulation amplitude possible was restricted to 0.5 mA, the  
328 threshold search procedure included the drop down in frequency to allow more granularity in  
329 threshold determination as described in the Methods. All stimulation amplitude, frequencies and  
330 percept descriptions at threshold are included in Tables 2 and 3.

331 *HD-ECoG and SEEG electrodes provide access to different cortical areas.*

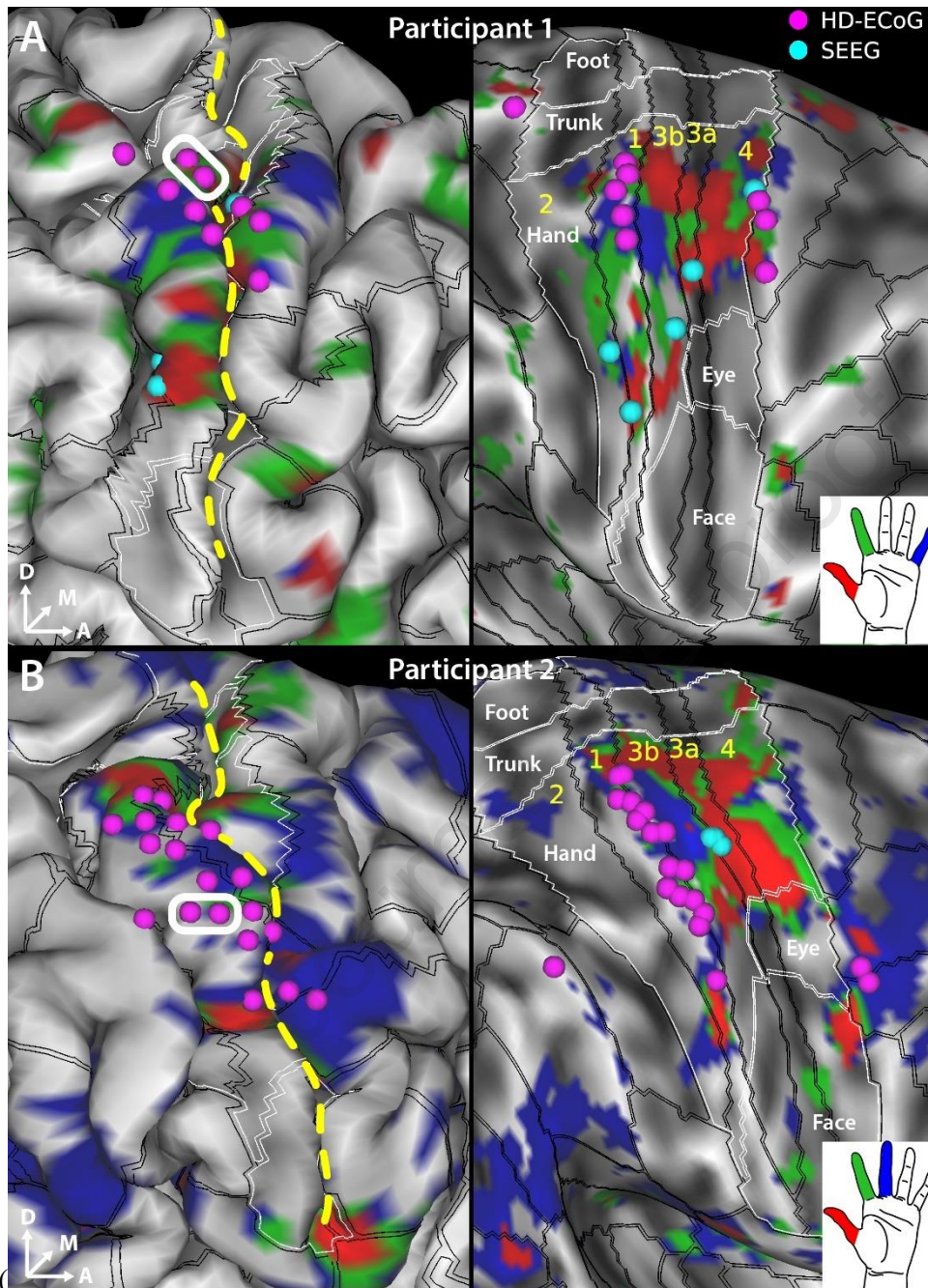
332 To locate the representation of the fingers in S1 (



333

334 Figure 1 insets), the participants performed button-press tasks using thumb (D1, red), index (D2,  
 335 green), and little finger (D5, blue, participant 1) or middle finger (D3, blue, participant 2) during  
 336 functional imaging. The motivation for including digits 1, 2, and 5 in participant 1 was to map the  
 337 extents of the hand while in participant 2, our motivation evolved to focus on the first three  
 338 digits, as they are functionally more important in grasping and manipulating objects. The fMRI

339 activation results were thresholded to optimize the visualization of topological features in area 3b



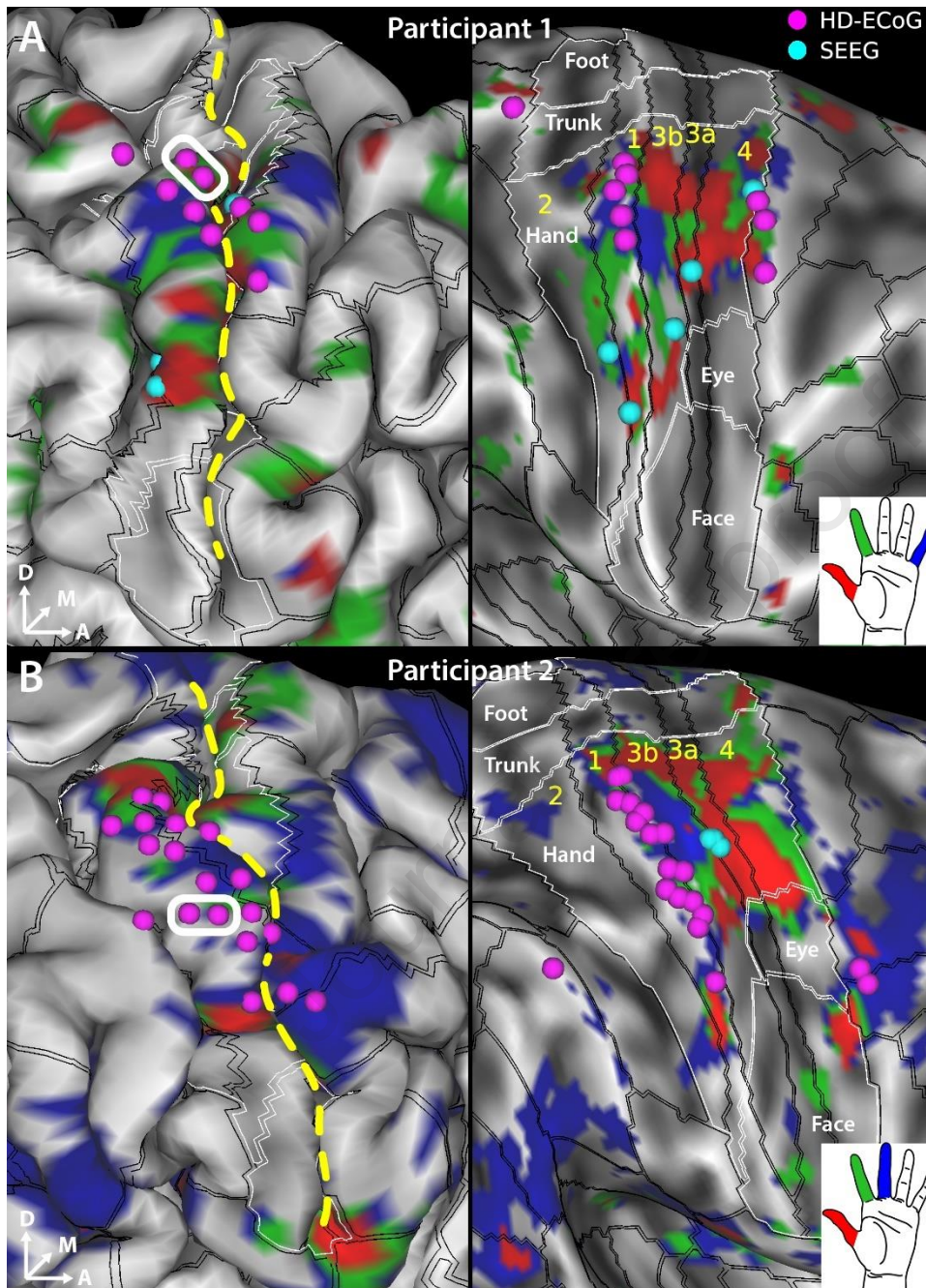
340

341 Figure 1, right panels), located on the posterior wall of the central sulcus, and overlaid (from top  
 342 to bottom without transparency: red, green, and blue) on group average cortical areal maps [40].  
 343 Figure S1 demonstrates that the group average cortical areal definitions align well with the  
 344 individual subject cortical myelin and thickness maps. Overlapping activation in area 4 (anterior  
 345 wall of the central sulcus) and 3a (fundus of the central sulcus) are evident (most of the blue and

346 a large portion of the green are hidden beneath the red color) in both participants. A  
347 topologically meaningful representation of D1, D2, and D3/D5 can be observed in the lateral-  
348 medial axis in area 3b in both participants. Interestingly, activation in regions medial to the  
349 D3/D5 representation can be observed in D1 (red) and D2 (green) tasks. Less consistent  
350 individual digit representations were observed in area 1 (postcentral gyrus), except for an  
351 overlapping activation in the lateral location of D1 for all finger tasks. Even less consistent or  
352 appreciable activations exist in area 2 at the chosen threshold level (Figure S2).

353         We were interested in further elucidating the digit representations in the sulcal and gyral  
354 areas of S1. Specifically, we wanted to determine whether electrical stimulation using SEEG  
355 depth electrodes can effectively target these digit representations in the sulcal areas of S1.  
356 Overlaying the electrodes that evoked sensations in the hand on top of the fMRI maps shows that  
357 the HD-ECoG electrodes (fuschia spheres in Fig. 1) appear to cluster in area 1 which covers the

358 apical surface of the postcentral gyrus. Meanwhile, the SEEG electrodes (cyan spheres in



359

360 Figure 1) that evoked sensory percepts in the hand, when projected to the cortical surface,  
 361 localize predominantly to the areas 3a and 3b of S1 which are located at the fundus and posterior  
 362 wall of the central sulcus, respectively. In case of SEEG, the electrode pairs always consisted of  
 363 adjacent electrodes within the same lead. The orientation of all HD-ECoG electrode pairs was

364 parallel to the example electrode pair shown for each participant in the Figure 1 (white  
365 rectangle).

366 *Fingertip percepts evoked by sulcal stimulation.*

367 We characterized the sensory percepts evoked by direct electrical stimulation of S1 gyral  
368 and sulcal areas using HD-ECoG or SEEG electrodes, respectively. In both participants,  
369 electrical stimulation was gradually ramped up until percept threshold was reached, at which  
370 point the participants described what they perceived. We observed that the percepts evoked by  
371 sulcal stimulation tended to be highly focal, often restricted to within a single segment of a  
372 finger, and often at the fingertips. The SEEG electrodes that evoke these percepts were  
373 predominantly located near the anterior wall of the postcentral gyrus (Figure 2, panels A and C;  
374 Figure S3). Meanwhile, the percepts evoked by gyral stimulation often extended over multiple  
375 segments of a digit or multiple digits (Figure 2, panels B and D). Interestingly, we observed a  
376 paucity in percepts restricted to fingertips alone when stimulating S1 gyral areas. As expected,  
377 the evoked percepts exhibit a somatotopical organization of the hand, with thumb percepts  
378 evoked by electrodes that were more laterally located, while percepts in the index and middle  
379 fingers and the wrist were evoked by electrodes that were more dorsal (Figure 2D).

380 *Focal and distal percepts evoked by sulcal stimulation.*

381 Comparing the areas enclosed by the sensory percepts showed that sulcal stimulation using  
382 SEEG electrodes evoked percepts that were significantly smaller than those evoked by gyral  
383 stimulation using HD-ECoG electrodes (Figure 3A,  $p=0.02$ , Wilcoxon ranksum test,  $\chi^2 = 5.57$ ).  
384 This suggests that the sensory percepts evoked by sulcal stimulation tend to be more focal in  
385 their spatial spread. Comparing the probability of occurrence of percepts of different sizes also  
386 showed significant skew towards percepts with smaller area in case of sulcal stimulation (Figure  
387 3B,  $p \ll 0.01$ , Kolmogorov-Smirnov test).

388 To evaluate if there was a difference in the location of the percepts evoked by gyral and  
389 sulcal stimulation, we determined the probability that an evoked percept covered a particular area  
390 of the hand. Figure 4 shows a probability of a percept covering a region of the hand normalized  
391 to the maximal number of percepts covering any area of the hand. Fingertips are most often  
392 covered by percepts evoked by SEEG-mediated sulcal stimulation (Figure 4A) while gyral  
393 stimulation evoked percepts cover the middle phalanges most often (Figure 4B). Percepts

394 covering the index fingertip sensation were evoked most often (evoked by 4 electrodes) followed  
395 by middle and ring fingertips (evoked by 3 electrodes). Given that 12 SEEG electrodes evoked  
396 sensations localized to the hand and wrist, percepts that spread over the fingertips constituted up  
397 to 25-30% of those evoked by SEEG electrodes located in the sulcal regions of S1. In  
398 comparison, only 6-12% of the percepts evoked by the electrodes locate on the postcentral gyrus  
399 (2-4 out of 31 electrodes) covered the fingertips while the most represented region of the hand  
400 were the middle phalanges of the fingers and the ulnar side of the hand (up to 30%).

401 *Cortical activity recorded during mechanical tactile stimuli.*

402 While implanted with SEEG electrodes, participant 2 also received mechanical tactile  
403 stimulation of the thumb, index and middle finger pads and the resultant neural activity in S1  
404 was recorded (see Figure S4). We aimed to further confirm the previously identified sulcal  
405 locations were involved in fingertip tactile sensation. We identified electrodes from which neural  
406 activity were recorded that showed a high degree of repeatability (mean correlation coefficient,  $r$   
407  $\geq 0.6$ ) among features in the high gamma band (100–500 Hz) across repeated cycles of  
408 mechanical stimulation, i.e., tapping of the fingertips. We show that sulcal electrodes recording  
409 stimulus evoked somatosensory activity were spatially clustered (Figure 5A). Interestingly, the  
410 sulcal electrodes that evoked a sensory percept in the hand overlapped or were located close to  
411 the sulcal electrodes that were activated by tactile stimulation of the fingertips (Figure 5B).

## 412 **Discussion**

413 In this study, we demonstrate that sulcal stimulation in human S1 evokes sensory  
414 percepts localized to the fingertips more often than gyral stimulation. SEEG electrodes provided  
415 an effective way to deliver targeted electrical stimulation to sulcal regions of S1. Using these  
416 electrodes, in two participants, we were able to evoke sensory percepts restricted to single  
417 segments of a digit, including fingertips and more focal than those evoked by gyral stimulation  
418 using HD-ECoG electrodes. We were also able to record neural correlates of mechanical tactile  
419 stimuli delivered at the fingertips on sulcal contacts that were spatially clustered. The findings in  
420 this study suggest that evoking fingertip percepts through intracortical stimulation would require  
421 accessing the sulcal regions of S1. Additionally, it shows the potential of electrodes targeted to  
422 the sulcal regions in providing intuitive and useful somatosensory feedback for dexterous hand  
423 movements in sensorimotor BCIs.

424 We used neuroimaging tools designed by the Human Connectome Project to elucidate the  
425 precise subregions of S1 in relation to electrode implantation. Though the fMRI activation maps  
426 highlight the somatotopic subregion corresponding to the hand area in S1, the cortical areas of S1  
427 are not clearly delineated. In this study, the intrinsic blood-oxygen-level-dependent (BOLD)  
428 point spread function at 3T, and the less well-defined finger task do not allow us to detect fMRI  
429 activation patterns of the distal (i.e., fingertip) vs proximal phalanges. However, previous studies  
430 with 7T fMRI have been able to localize representation of the fingertips in S1 [18]. The group  
431 average cortical parcellations based on T1w/T2w-based myelin content and cortical thickness  
432 maps could effectively guide implantation of SEEG electrodes to target the finger representations  
433 in S1.

434 The well-known somatotopy of the human S1 represents the digits D1 (thumb) to D5  
435 (little finger) in lateral-to-medial succession from the lateral border of the upper extremity  
436 subregion. Such somatotopic mapping was characteristically depicted in the task fMRI  
437 activations in area 3b in both participants [20,21], notwithstanding the possibility of visually-  
438 driven contribution [57], while thenar (muscles under the base of the thumb) and palm sensation  
439 during finger tapping likely account for the activations observed in areas medial to the D5  
440 representation. We interpret the overlapping activations from all fingers within the representation  
441 of D1 in area 1 as an inadvertent result of increased counter-balance pressure of the thumb  
442 pressing against the surface underneath, while the other fingers were lifted during finger tapping.  
443 Among the fingers, the thumb shows the most consistent and distinct representation in the  
444 expected somatotopic subregion. This is consistent with the relatively isolated anatomical  
445 structure of D1 from other fingers. The less consistent and focal representation of the other  
446 fingers are potentially due to a couple of reasons. First, unlike other elegant sensory task designs  
447 with dedicated tactile or electrical stimulation devices for each finger, sensory activations from  
448 common motor tasks are inherently imprecise despite best-efforts in task instruction and subject  
449 compliance. Second, the isolation of single digit motion is much more difficult for the rest of the  
450 digits than the thumb.

451 Our observation of sulcal stimulation in human S1 evoking fingertip percepts more often  
452 than gyral stimulation is in agreement with functional imaging studies that have predominantly  
453 localized fingertip representation to the posterior wall of the central sulcus (area 3b) and  
454 occasionally at the crown of the postcentral gyrus [18–21,28]. With the mirror-reversal of

455 representation occurring at the area 3b-1 border, the representation of fingertips might still  
456 extend into the posterior regions of the postcentral gyrus as shown by some imaging [25,26,30]  
457 and recent stimulation studies [27]. However, in our study, we had only two SEEG contacts  
458 located deep in the postcentral sulcus in one participant that evoked percepts in the hand. None  
459 of the electrodes located in the posterior regions of the postcentral gyrus evoked fingertip  
460 percepts. It might be the case that the fingertip representations on the crown of the postcentral  
461 gyrus are small and require extremely precise targeting, while they are more extensive within the  
462 central sulcus and hence, easily accessible with SEEG electrodes.

463         Recently, both microelectrode arrays and ECoG grid electrodes have been used to  
464 provide artificial sensory feedback. While individual microelectrode array contacts evoke highly  
465 focal percepts restricted to individual phalanges, by activating very closely spaced cortical  
466 locations they provide only limited coverage of the hand, often restricted to only a few phalanges  
467 over two or three fingers [10–12]. Such high degree of anatomical overlap among the evoked  
468 percepts restricts the amount of sensory information that can be conveyed. Meanwhile, with  
469 larger size and inter-contact spacing when compared to microelectrode arrays, HD-ECoG  
470 electrodes elicit sensory percepts that tend to cover either multiple phalanges or entire digits  
471 [13,15,58]. Additionally, with the capability to record or modulate the neural activity of neurons  
472 that lie within 1-2 mm below the cortical surface [59], these electrodes provide access to only the  
473 gyral surfaces of the cortex.

474         With the potential to reach sulcal areas of the cortex, SEEG electrodes provide a unique  
475 advantage of being able to evoke tactile sensations that are perceived to emanate from the  
476 fingers, particularly fingertips. A recent study has reported being able to target fingertip  
477 representations on the postcentral gyrus using microelectrode arrays in a patient with SCI [12].  
478 However, such precise targeting was possible only after performing extensive intraoperative  
479 mapping of neural responses in S1 to peripheral stimulation of the fingertips relying on the  
480 relatively intact residual sensory pathways. Such an approach based on evoked responses in S1  
481 might not be feasible in case of other potential users of BCI with more severe loss of function. It  
482 is well established that motor imagery can be used to identify the hand area of the motor cortex  
483 in people with tetraplegia [9]. Moreover, in able-bodied individuals, motor imagery has been  
484 shown to activate both primary motor and somatosensory cortices [60]. In addition, the finger  
485 regions of the primary motor cortex and somatosensory cortex are juxtaposed against each other

486 across the central sulcus [61]. We therefore expect that motor imagery alone can help localize the  
487 finger regions in the somatosensory cortex in people with high-level tetraplegia guiding  
488 minimally invasive SEEG implantation.

489 SEEG electrodes have recently been gaining favor for seizure onset localization as well  
490 as for mapping eloquent areas of the cortex in case of medically refractory epilepsy [32]. In  
491 contrast to other intracranial electrodes that require burr holes or large craniotomies for  
492 implantation, SEEG electrodes can be implanted using a minimally invasive approach via a 1–2  
493 mm craniostomy [31]. The minimally invasive approach for their implantation reduces the risk of  
494 hemorrhage and infection to 1% and 0.8% respectively from that of 4% and 2.3% for subdural  
495 electrodes such as ECoG grids [38,39].

496 In this study, all stimulation was done using a bipolar configuration involving adjacent  
497 electrodes. While the inter-contact spacing are comparable (4–5 mm in HD-ECoG vs 4.43 mm in  
498 SEEG) between the two electrode types, the surface area of SEEG electrodes ( $\sim 5 \text{ mm}^2$ ) are  
499 almost twice that of HD-ECoG electrodes ( $\sim 3 \text{ mm}^2$ ). Combined with the lack of directionality,  
500 SEEG electrodes should potentially activate a wider area of cortex evoking bigger or mixed  
501 percepts. The high-level of two-point discrimination at fingertips is due to the high density of  
502 mechanoreceptors as well as smaller receptive fields for fingertips in S1. Stimulating cortical  
503 areas with small receptive fields have been shown to evoke smaller percepts in the human visual  
504 cortex [62]. A similar relationship between receptive field and percept size in S1 would enable  
505 cortical stimulation targeted at fingertip representations to evoke smaller percepts. It is possible  
506 that the difference in receptive field sizes between gyral and sulcal areas are a stronger  
507 determining factor of the evoked percept size than the electrode form factor.

508 Future studies should explore denser, smaller and even directional SEEG electrodes that  
509 could restrict the effective volume of cortical tissue that is activated and thus, evoke more focal  
510 percepts. However, higher current density and the potential tissue damage are factors that will  
511 have to be considered as well. Another potential limitation of the current study is the low number  
512 of participants. However, we specifically included only those participants who had at least 2 or  
513 more electrodes in S1 that evoked percepts in the hand area. Moreover, the two participants  
514 included were implanted with both types of electrodes enabling a within-patient comparison.  
515 Proprioception is potentially as critical as tactile percepts for dexterous motor control. We did

516 not explicitly explore evoking proprioceptive percepts in this study. Non-human primate studies  
517 have shown that area 3a, located at the fundus of the central sulcus, has the largest incidence of  
518 proprioceptive cells [63]. SEEG electrodes present one of the best avenues to explore the  
519 effectiveness of evoking proprioceptive percepts by stimulating area 3a.

520         The MCC (repeatability metric) of recorded neural activity during mechanical tactile  
521 stimulation of the fingertips highlighted SEEG contacts that were either identical or adjacent to  
522 those that evoked percepts in the hand. This overlap between receptive fields of mechanical  
523 stimuli at the periphery and the percept field evoked by cortical stimulation was potentially due  
524 to the relatively large size of the electrodes resulting in both activation as well as recording of  
525 neural activity of a relatively large pool of local neurons as compared to microelectrode arrays.  
526 This further supports that the sulcal locations identified during electrical stimulation are indeed  
527 related to and important in tactile sensory restoration. This could also potentially provide a safer  
528 way to map eloquent cortex avoiding direct electrical stimulation which could trigger after-  
529 discharges or seizure activity [64] as well as for recording task-related, highly relevant neural  
530 activity for BCI applications.

531         Thus, we have shown that the representation of fingertips is readily accessible on the  
532 posterior wall of the central sulcus using SEEG electrodes. This suggests that sulcal stimulation  
533 mediated by SEEG electrodes offer a highly viable alternative to the current approaches  
534 restricted to gyral stimulation for restoring somatosensation. Future technical developments that  
535 will allow tightly spaced electrodes are important for greater success and efficacy. A recent  
536 review explored the potential of SEEG electrodes in BCI applications for decoding intended  
537 movement [65]. Combined with our findings on sulcal stimulation being able to provide highly  
538 focal and relevant somatosensory feedback, we venture that SEEG electrodes can potentially  
539 become an established approach for sensorimotor restoration in closed loop BCI applications.  
540 Moreover, with the ability of reaching deeper structures of the cortex, SEEG-mediated  
541 stimulation can potentially mitigate sensorimotor deficits arising due to even subcortical strokes  
542 along the cortico-spinal tract.

#### 543 **Acknowledgements**

544 We would like to thank our participants for their extraordinary commitment to this study, their  
545 patience with the experiments, and the deep insights provided by them, the clinicians and

546 researchers at Feinstein Institutes for Medical Research. We would also like to thank Kevin  
547 Tracey, MD for providing critical inputs on the manuscript.

548 **Funding**

549 This study was funded through support provided by Feinstein Institutes for Medical Research at  
550 Northwell Health and partly funded by Empire Clinical Research Investigator Program (ECRIP)  
551 Fellowship of which SB was a recipient. MFG was supported by NIH R01MH060974.

Journal Pre-proof

552 **References**

- 553 [1] Armour BS, Courtney-Long EA, Fox MH, Fredine H, Cahill A. Prevalence and Causes of Paralysis-  
 554 United States, 2013. *American Journal of Public Health* 2016;106:1855–7.  
 555 <https://doi.org/10.2105/AJPH.2016.303270>.
- 556 [2] NSCISC. Facts and Figures at a Glance 2020.
- 557 [3] Zhou B, Lu Y, Hajifathalian K, Bentham J, Di Cesare M, Danaei G, et al. Worldwide trends in  
 558 diabetes since 1980: a pooled analysis of 751 population-based studies with 4·4 million  
 559 participants. *The Lancet* 2016;387:1513–30. [https://doi.org/10.1016/S0140-6736\(16\)00618-8](https://doi.org/10.1016/S0140-6736(16)00618-8).
- 560 [4] Ennis SL, Galea MP, O’Neal DN, Dodson MJ. Peripheral neuropathy in the hands of people with  
 561 diabetes mellitus. *Diabetes Research and Clinical Practice* 2016;119:23–31.  
 562 <https://doi.org/10.1016/j.diabres.2016.06.010>.
- 563 [5] Rothwell JC, Traub MM, Day BL, Obeso JA, Thomas PK, Marsden CD. Manual Motor Performance in  
 564 a Deafferented Man. *Brain* 1982;105:515–42. <https://doi.org/10.1093/brain/105.3.515>.
- 565 [6] Monzée J, Lamarre Y, Smith AM. The Effects of Digital Anesthesia on Force Control Using a  
 566 Precision Grip. *Journal of Neurophysiology* 2003;89:672–83.  
 567 <https://doi.org/10.1152/jn.00434.2001>.
- 568 [7] Hochberg LR, Bacher D, Jarosiewicz B, Masse NY, Simeral JD, Vogel J, et al. Reach and grasp by  
 569 people with tetraplegia using a neurally controlled robotic arm. *Nature* 2012;485:372–5.  
 570 <https://doi.org/10.1038/nature11076>.
- 571 [8] Collinger JL, Wodlinger B, Downey JE, Wang W, Tyler-Kabara EC, Weber DJ, et al. High-  
 572 performance neuroprosthetic control by an individual with tetraplegia. *The Lancet* 2013;381:557–  
 573 64. [https://doi.org/10.1016/S0140-6736\(12\)61816-9](https://doi.org/10.1016/S0140-6736(12)61816-9).
- 574 [9] Bouton CE, Shaikhouni A, Annetta NV, Bockbrader MA, Friedenber DA, Nielson DM, et al.  
 575 Restoring cortical control of functional movement in a human with quadriplegia. *Nature*  
 576 2016;533:247–50. <https://doi.org/10.1038/nature17435>.
- 577 [10] Flesher SN, Collinger JL, Foldes ST, Weiss JM, Downey JE, Tyler-Kabara EC, et al. Intracortical  
 578 microstimulation of human somatosensory cortex. *Science Translational Medicine*  
 579 2016;8:361ra141. <https://doi.org/10.1126/scitranslmed.aaf8083>.
- 580 [11] Armenta Salas M, Bashford L, Kellis S, Jafari M, Jo H, Kramer D, et al. Proprioceptive and cutaneous  
 581 sensations in humans elicited by intracortical microstimulation. *ELife* 2018;7:e32904.  
 582 <https://doi.org/10.7554/eLife.32904>.
- 583 [12] Fifer MS, McMullen DP, Thomas TM, Osborn LE, Nickl RW, Candrea DN, et al. Intracortical  
 584 Microstimulation Elicits Human Fingertip Sensations. *MedRxiv* 2020:2020.05.29.20117374.  
 585 <https://doi.org/10.1101/2020.05.29.20117374>.
- 586 [13] Hiremath SV, Tyler-Kabara EC, Wheeler JJ, Moran DW, Gaunt RA, Collinger JL, et al. Human  
 587 perception of electrical stimulation on the surface of somatosensory cortex. *PLoS One*  
 588 2017;12:e0176020. <https://doi.org/10.1371/journal.pone.0176020>.
- 589 [14] Lee B, Kramer D, Armenta Salas M, Kellis S, Brown D, Dobrev T, et al. Engineering Artificial  
 590 Somatosensation Through Cortical Stimulation in Humans. *Frontiers in Systems Neuroscience*  
 591 2018;12:24. <https://doi.org/10.3389/fnsys.2018.00024>.
- 592 [15] Kramer DR, Lee MB, Barbaro M, Gogia AS, Peng T, Liu C, et al. Mapping of primary somatosensory  
 593 cortex of the hand area using a high-density electrocorticography grid for closed-loop brain  
 594 computer interface. *J Neural Eng* 2020. <https://doi.org/10.1088/1741-2552/ab7c8e>.
- 595 [16] Flesher SN, Downey JE, Weiss JM, Hughes CL, Herrera AJ, Tyler-Kabara EC, et al. Restored tactile  
 596 sensation improves neuroprosthetic arm control. *BioRxiv* 2019:653428.  
 597 <https://doi.org/10.1101/653428>.

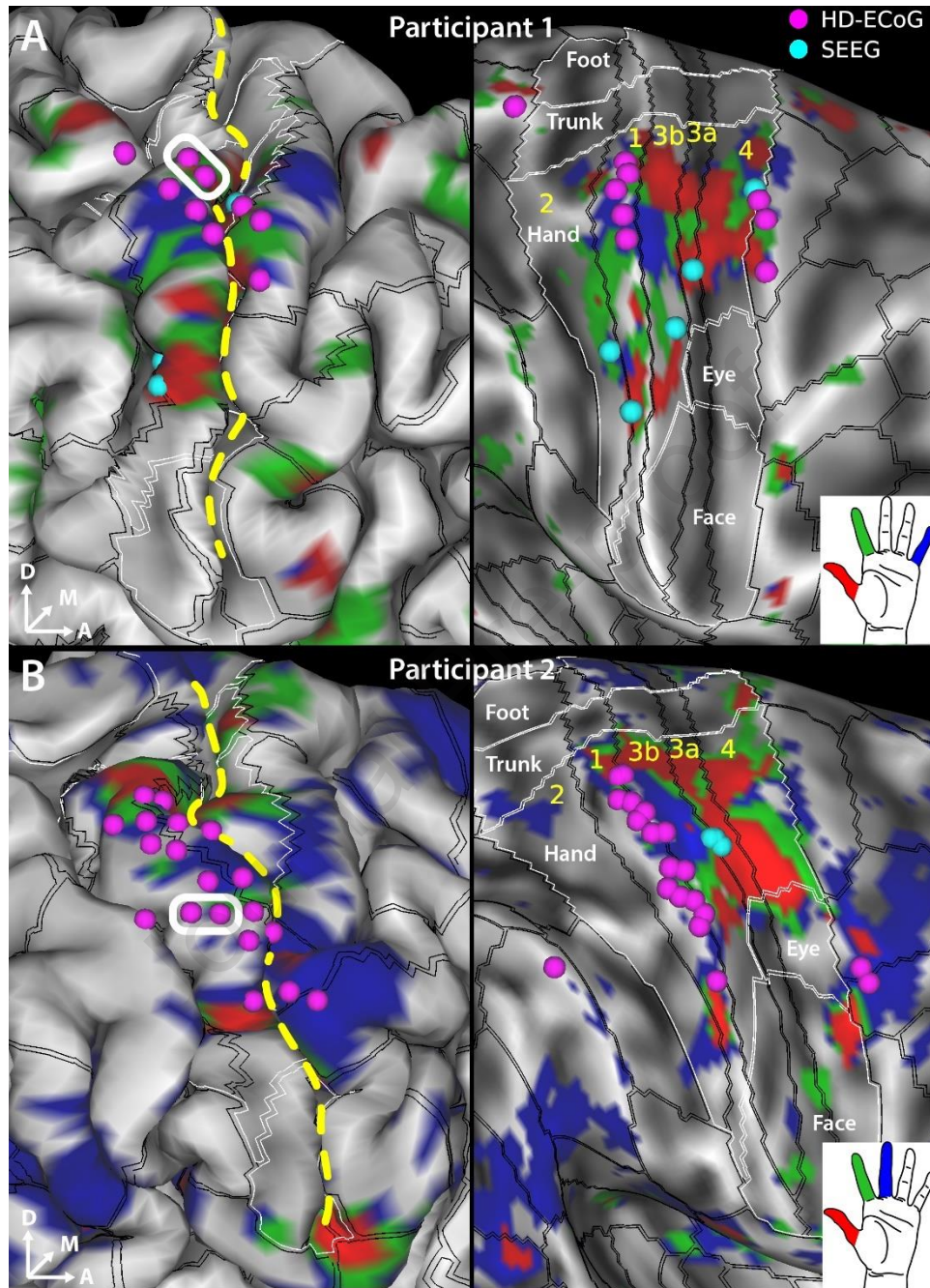
- 598 [17] Johansson RS, Flanagan JR. Coding and use of tactile signals from the fingertips in object  
599 manipulation tasks. *Nature Reviews Neuroscience* 2009;10:345–59.  
600 <https://doi.org/10.1038/nrn2621>.
- 601 [18] Sanchez-Panchuelo RM, Besle J, Beckett A, Bowtell R, Schluppeck D, Francis S. Within-Digit  
602 Functional Parcellation of Brodmann Areas of the Human Primary Somatosensory Cortex Using  
603 Functional Magnetic Resonance Imaging at 7 Tesla. *J Neurosci* 2012;32:15815–22.  
604 <https://doi.org/10.1523/JNEUROSCI.2501-12.2012>.
- 605 [19] Martuzzi R, van der Zwaag W, Farthouat J, Gruetter R, Blanke O. Human finger somatotopy in  
606 areas 3b, 1, and 2: A 7T fMRI study using a natural stimulus. *Human Brain Mapping* 2014;35:213–  
607 26. <https://doi.org/10.1002/hbm.22172>.
- 608 [20] Kolasinski J, Makin TR, Jbabdi S, Clare S, Stagg CJ, Johansen-Berg H. Investigating the Stability of  
609 Fine-Grain Digit Somatotopy in Individual Human Participants. *J Neurosci* 2016;36:1113–27.  
610 <https://doi.org/10.1523/JNEUROSCI.1742-15.2016>.
- 611 [21] Sanchez Panchuelo RM, Ackerley R, Glover PM, Bowtell RW, Wessberg J, Francis ST, et al. Mapping  
612 quantal touch using 7 Tesla functional magnetic resonance imaging and single-unit intraneural  
613 microstimulation. *ELife* 2016;5:e12812. <https://doi.org/10.7554/eLife.12812>.
- 614 [22] Merzenich MM, Kaas JH, Sur M, Lin C-S. Double representation of the body surface within  
615 cytoarchitectonic area 3b and 1 in “SI” in the owl monkey (*aotus trivirgatus*). *Journal of*  
616 *Comparative Neurology* 1978;181:41–73. <https://doi.org/10.1002/cne.901810104>.
- 617 [23] Kaas JH, Nelson RJ, Sur M, Lin CS, Merzenich MM. Multiple representations of the body within the  
618 primary somatosensory cortex of primates. *Science* 1979;204:521–3.  
619 <https://doi.org/10.1126/science.107591>.
- 620 [24] Nelson RJ, Sur M, Felleman DJ, Kaas JH. Representations of the body surface in postcentral parietal  
621 cortex of *Macaca fascicularis*. *Journal of Comparative Neurology* 1980;192:611–43.  
622 <https://doi.org/10.1002/cne.901920402>.
- 623 [25] Blankenburg F, Ruben J, Meyer R, Schwiemann J, Villringer A. Evidence for a Rostral-to-Caudal  
624 Somatotopic Organization in Human Primary Somatosensory Cortex with Mirror-reversal in Areas  
625 3b and 1. *Cereb Cortex* 2003;13:987–93. <https://doi.org/10.1093/cercor/13.9.987>.
- 626 [26] Nelson AJ, Chen R. Digit Somatotopy within Cortical Areas of the Postcentral Gyrus in Humans.  
627 *Cereb Cortex* 2008;18:2341–51. <https://doi.org/10.1093/cercor/bhm257>.
- 628 [27] Roux F-E, Djidjeli I, Durand J-B. Functional architecture of the somatosensory homunculus detected  
629 by electrostimulation. *The Journal of Physiology* 2018;596:941–56.  
630 <https://doi.org/10.1113/JP275243>.
- 631 [28] Schweisfurth MA, Frahm J, Schweizer R. Individual fMRI maps of all phalanges and digit bases of all  
632 fingers in human primary somatosensory cortex. *Front Hum Neurosci* 2014;8.  
633 <https://doi.org/10.3389/fnhum.2014.00658>.
- 634 [29] Schweisfurth MA, Frahm J, Schweizer R. Individual left-hand and right-hand intra-digit  
635 representations in human primary somatosensory cortex. *Eur J Neurosci* 2015;42:2155–63.  
636 <https://doi.org/10.1111/ejn.12978>.
- 637 [30] O’Neill GC, Sengupta A, Asghar M, Barratt EL, Besle J, Schluppeck D, et al. A probabilistic atlas of  
638 finger dominance in the primary somatosensory cortex. *NeuroImage* 2020;217:116880.  
639 <https://doi.org/10.1016/j.neuroimage.2020.116880>.
- 640 [31] Gholipour T, Koubeissi MZ, Shields DC. Stereotactic electroencephalography. *Clinical Neurology*  
641 *and Neurosurgery* 2020;189:105640. <https://doi.org/10.1016/j.clineuro.2019.105640>.
- 642 [32] Abou-Al-Shaar H, Brock AA, Kundu B, Englot DJ, Rolston JD. Increased nationwide use of  
643 stereoencephalography for intracranial epilepsy electroencephalography recordings. *Journal of*  
644 *Clinical Neuroscience* 2018;53:132–4. <https://doi.org/10.1016/j.jocn.2018.04.064>.

- 645 [33] Balestrini S, Francione S, Mai R, Castana L, Casaceli G, Marino D, et al. Multimodal responses  
646 induced by cortical stimulation of the parietal lobe: a stereo-electroencephalography study. *Brain*  
647 2015;138:2596–607. <https://doi.org/10.1093/brain/awv187>.
- 648 [34] Mazzola L, Royet J-P, Catenoix H, Montavont A, Isnard J, Mauguière F. Gustatory and olfactory  
649 responses to stimulation of the human insula. *Annals of Neurology* 2017;82:360–70.  
650 <https://doi.org/10.1002/ana.25010>.
- 651 [35] Britton JW. Electrical Stimulation Mapping with Stereo-EEG Electrodes. *Journal of Clinical*  
652 *Neurophysiology* 2018;35:110–4. <https://doi.org/10.1097/WNP.0000000000000443>.
- 653 [36] Young JJ, Coulehan K, Fields MC, Yoo JY, Marcuse LV, Jette N, et al. Language mapping using  
654 electrocorticography versus stereoelectroencephalography: A case series. *Epilepsy & Behavior*  
655 2018;84:148–51. <https://doi.org/10.1016/j.yebeh.2018.04.032>.
- 656 [37] Arya R, Ervin B, Holloway T, Dudley J, Horn PS, Buroker J, et al. Electrical stimulation sensorimotor  
657 mapping with stereo-EEG. *Clinical Neurophysiology* 2020;131:1691–701.  
658 <https://doi.org/10.1016/j.clinph.2020.04.159>.
- 659 [38] Mullin JP, Shriver M, Alomar S, Najm I, Bulacio J, Chauvel P, et al. Is SEEG safe? A systematic review  
660 and meta-analysis of stereo-electroencephalography-related complications. *Epilepsia*  
661 2016;57:386–401. <https://doi.org/10.1111/epi.13298>.
- 662 [39] Arya R, Mangano FT, Horn PS, Holland KD, Rose DF, Glauser TA. Adverse events related to  
663 extraoperative invasive EEG monitoring with subdural grid electrodes: A systematic review and  
664 meta-analysis. *Epilepsia* 2013;54:828–39. <https://doi.org/10.1111/epi.12073>.
- 665 [40] Glasser MF, Coalson TS, Robinson EC, Hacker CD, Harwell J, Yacoub E, et al. A multi-modal  
666 parcellation of human cerebral cortex. *Nature* 2016;536:171–8.  
667 <https://doi.org/10.1038/nature18933>.
- 668 [41] Setsompop K, Gagoski BA, Polimeni JR, Witzel T, Wedeen VJ, Wald LL. Blipped-controlled aliasing in  
669 parallel imaging for simultaneous multislice echo planar imaging with reduced g-factor penalty.  
670 *Magn Reson Med* 2012;67:1210–24. <https://doi.org/10.1002/mrm.23097>.
- 671 [42] Xu J, Moeller S, Auerbach EJ, Strupp J, Smith SM, Feinberg DA, et al. Evaluation of slice  
672 accelerations using multiband echo planar imaging at 3 T. *Neuroimage* 2013;83:991–1001.  
673 <https://doi.org/10.1016/j.neuroimage.2013.07.055>.
- 674 [43] Glasser MF, Sotiropoulos SN, Wilson JA, Coalson TS, Fischl B, Andersson JL, et al. The Minimal  
675 Preprocessing Pipelines for the Human Connectome Project. *Neuroimage* 2013;80:105–24.  
676 <https://doi.org/10.1016/j.neuroimage.2013.04.127>.
- 677 [44] Robinson EC, Jbabdi S, Glasser MF, Andersson J, Burgess GC, Harms MP, et al. MSM: A new flexible  
678 framework for Multimodal Surface Matching. *NeuroImage* 2014;100:414–26.  
679 <https://doi.org/10.1016/j.neuroimage.2014.05.069>.
- 680 [45] Robinson EC, Garcia K, Glasser MF, Chen Z, Coalson TS, Makropoulos A, et al. Multimodal surface  
681 matching with higher-order smoothness constraints. *NeuroImage* 2018;167:453–65.  
682 <https://doi.org/10.1016/j.neuroimage.2017.10.037>.
- 683 [46] Griffanti L, Salimi-Khorshidi G, Beckmann CF, Auerbach EJ, Douaud G, Sexton CE, et al. ICA-based  
684 artefact removal and accelerated fMRI acquisition for improved resting state network imaging.  
685 *NeuroImage* 2014;95:232–47. <https://doi.org/10.1016/j.neuroimage.2014.03.034>.
- 686 [47] Salimi-Khorshidi G, Douaud G, Beckmann CF, Glasser MF, Griffanti L, Smith SM. Automatic  
687 denoising of functional MRI data: Combining independent component analysis and hierarchical  
688 fusion of classifiers. *NeuroImage* 2014;90:449–68.  
689 <https://doi.org/10.1016/j.neuroimage.2013.11.046>.
- 690 [48] Glasser MF, Coalson TS, Bijsterbosch JD, Harrison SJ, Harms MP, Anticevic A, et al. Using temporal  
691 ICA to selectively remove global noise while preserving global signal in functional MRI data.  
692 *NeuroImage* 2018;181:692–717. <https://doi.org/10.1016/j.neuroimage.2018.04.076>.

- 693 [49] Woolrich MW, Ripley BD, Brady M, Smith SM. Temporal Autocorrelation in Univariate Linear  
694 Modeling of fMRI Data. *NeuroImage* 2001;14:1370–86. <https://doi.org/10.1006/nimg.2001.0931>.
- 695 [50] Groppe DM, Bickel S, Dykstra AR, Wang X, Mégevand P, Mercier MR, et al. iELVis: An open source  
696 MATLAB toolbox for localizing and visualizing human intracranial electrode data. *Journal of*  
697 *Neuroscience Methods* 2017;281:40–8. <https://doi.org/10.1016/j.jneumeth.2017.01.022>.
- 698 [51] Fischl B. FreeSurfer. *NeuroImage* 2012;62:774–81.  
699 <https://doi.org/10.1016/j.neuroimage.2012.01.021>.
- 700 [52] Hamberger MJ, Williams AC, Schevon CA. Extraoperative neurostimulation mapping: Results from  
701 an international survey of epilepsy surgery programs. *Epilepsia* 2014;55:933–9.  
702 <https://doi.org/10.1111/epi.12644>.
- 703 [53] Bouton C, Bhagat N, Chandrasekaran S, Herrero J, Markowitz N, Espinal E, et al. Identifying and  
704 Decoding Temporally Correlated Neural Patterns in the Brain to Accurately Predict Individual  
705 Finger Movement and Tactile Stimuli of the Human Hand Using Stereoelectroencephalography.  
706 *MedRxiv* 2021:2021.04.06.21255006. <https://doi.org/10.1101/2021.04.06.21255006>.
- 707 [54] Avanzini P, Abdollahi RO, Sartori I, Caruana F, Pelliccia V, Casaceli G, et al. Four-dimensional maps  
708 of the human somatosensory system. *Proc Natl Acad Sci USA* 2016;113:E1936–43.  
709 <https://doi.org/10.1073/pnas.1601889113>.
- 710 [55] Ray S, Crone NE, Niebur E, Franaszczuk PJ, Hsiao SS. Neural Correlates of High-Gamma Oscillations  
711 (60–200 Hz) in Macaque Local Field Potentials and Their Potential Implications in  
712 Electroconvulsive Therapy. *Journal of Neuroscience* 2008;28:11526–36.  
713 <https://doi.org/10.1523/JNEUROSCI.2848-08.2008>.
- 714 [56] Ray S, Hsiao SS, Crone NE, Franaszczuk PJ, Niebur E. Effect of Stimulus Intensity on the Spike-Local  
715 Field Potential Relationship in the Secondary Somatosensory Cortex. *Journal of Neuroscience*  
716 2008;28:7334–43. <https://doi.org/10.1523/JNEUROSCI.1588-08.2008>.
- 717 [57] Kuehn E, Haggard P, Villringer A, Pleger B, Sereno MI. Visually-Driven Maps in Area 3b. *J Neurosci*  
718 2018;38:1295–310. <https://doi.org/10.1523/JNEUROSCI.0491-17.2017>.
- 719 [58] Kramer DR, Kellis S, Barbaro M, Salas MA, Nune G, Liu CY, et al. Technical considerations for  
720 generating somatosensation via cortical stimulation in a closed-loop sensory/motor brain-  
721 computer interface system in humans. *Journal of Clinical Neuroscience* 2019;63:116–21.  
722 <https://doi.org/10.1016/j.jocn.2019.01.027>.
- 723 [59] Freeman WJ, Rogers LJ, Holmes MD, Silbergeld DL. Spatial spectral analysis of human  
724 electrocorticograms including the alpha and gamma bands. *Journal of Neuroscience Methods*  
725 2000;95:111–21. [https://doi.org/10.1016/S0165-0270\(99\)00160-0](https://doi.org/10.1016/S0165-0270(99)00160-0).
- 726 [60] Stippich C, Ochmann H, Sartor K. Somatotopic mapping of the human primary sensorimotor cortex  
727 during motor imagery and motor execution by functional magnetic resonance imaging.  
728 *Neuroscience Letters* 2002;331:50–4. [https://doi.org/10.1016/S0304-3940\(02\)00826-1](https://doi.org/10.1016/S0304-3940(02)00826-1).
- 729 [61] Huber L, Finn ES, Handwerker DA, Bönstrup M, Glen DR, Kashyap S, et al. Sub-millimeter fMRI  
730 reveals multiple topographical digit representations that form action maps in human motor cortex.  
731 *NeuroImage* 2020;208:116463. <https://doi.org/10.1016/j.neuroimage.2019.116463>.
- 732 [62] Winawer J, Parvizi J. Linking Electrical Stimulation of Human Primary Visual Cortex, Size of Affected  
733 Cortical Area, Neuronal Responses, and Subjective Experience. *Neuron* 2016;92:1213–9.  
734 <https://doi.org/10.1016/j.neuron.2016.11.008>.
- 735 [63] Kim SS, Gomez-Ramirez M, Thakur PH, Hsiao SS. Multimodal Interactions between Proprioceptive  
736 and Cutaneous Signals in Primary Somatosensory Cortex. *Neuron* 2015;86:555–66.  
737 <https://doi.org/10.1016/j.neuron.2015.03.020>.
- 738 [64] Ritaccio AL, Brunner P, Schalk G. Electrical Stimulation Mapping of the Brain: Basic Principles and  
739 Emerging Alternatives. *Journal of Clinical Neurophysiology* 2018;35:86–97.  
740 <https://doi.org/10.1097/WNP.0000000000000440>.

- 741 [65] Herff C, Krusienski DJ, Kubben P. The Potential of Stereotactic-EEG for Brain-Computer Interfaces:  
742 Current Progress and Future Directions. *Front Neurosci* 2020;14:123.  
743 <https://doi.org/10.3389/fnins.2020.00123>.  
744

Journal Pre-proof

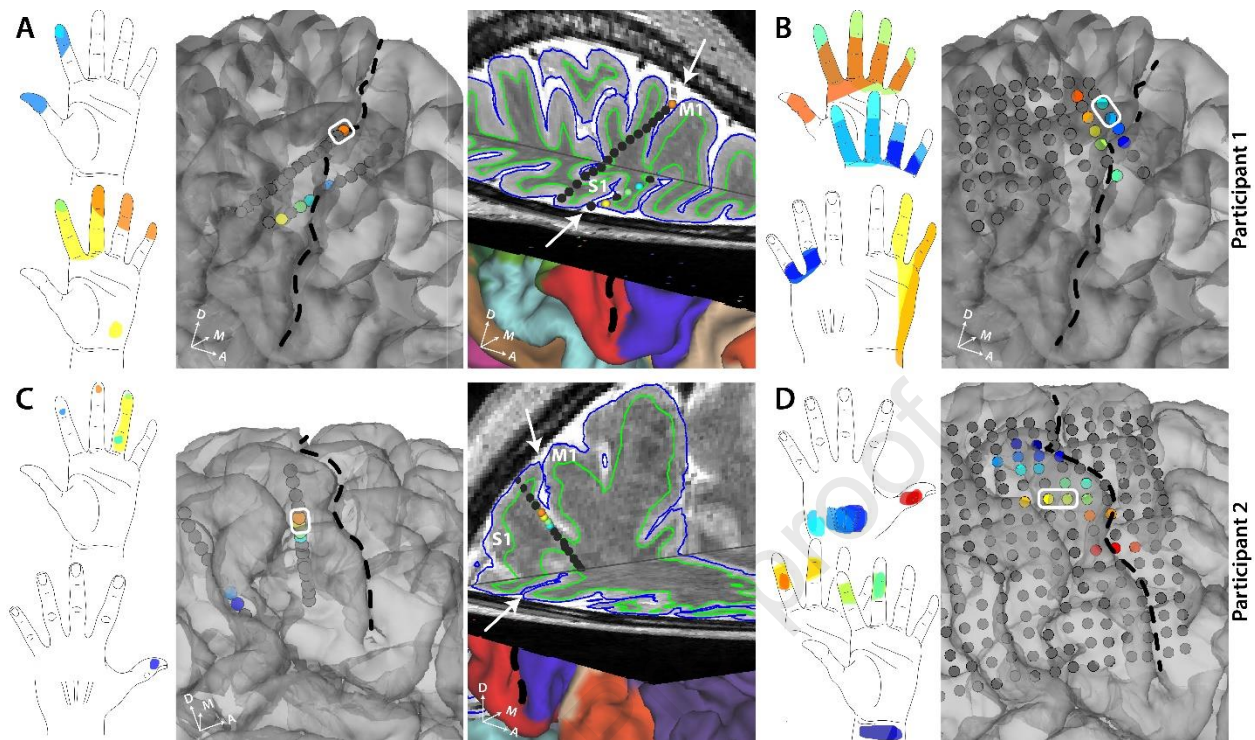
745 **Figures**

746

747 **Figure 1. fMRI activation maps for individual digits and electrode sites evoking sensory**  
 748 **percepts in the hand region upon electrical stimulation.** Sensorimotor cortex activation map  
 749 shown in **A.** for digits D1 (red), D2 (green) and D5 (blue) in participant 1 and in **B.** for digits D1  
 750 (red), D2 (green) and D3 (blue) in participant 2. SEEG (cyan spheres) and HD-ECoG (fuchsia  
 751 spheres) electrodes that evoked at least one sensory percept in the hand area are overlaid over the

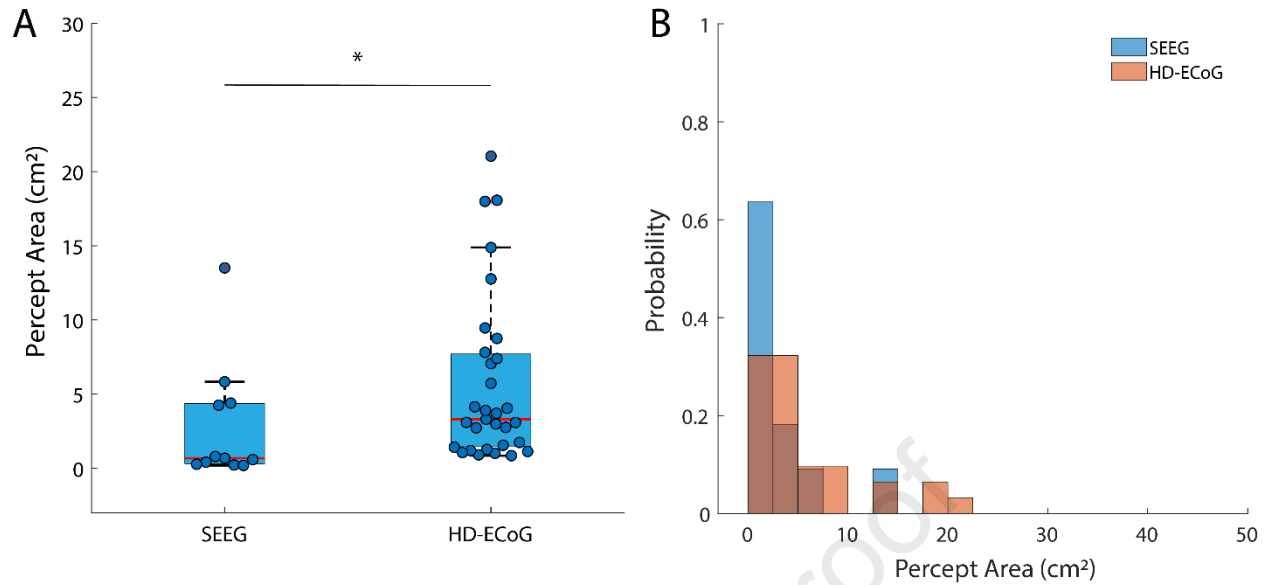
752 pial surface (left panels) and over the “very-inflated” representation of the cortical surface (right  
753 panels). An example bipolar electrode for HD-ECoG is shown (white rectangle). The black lines  
754 overlaid on the cortical surface delineate the cortical areal boundaries outside of sensorimotor  
755 cortex, and sensorimotor subregional boundaries inside sensorimotor cortex as derived from the  
756 HCP S1200 group average parcellation [40] based on myelin and cortical thickness maps and are  
757 labeled in yellow letters. The white lines demarcate the labeled somatotopic sensorimotor  
758 subregions based on resting state and task-based fMRI. The sensorimotor subareas are denoted  
759 by the intersection of the black and white boundaries. Gray shading denotes curvature of the  
760 cortical surface. Dashed yellow line denotes the central sulcus.

761



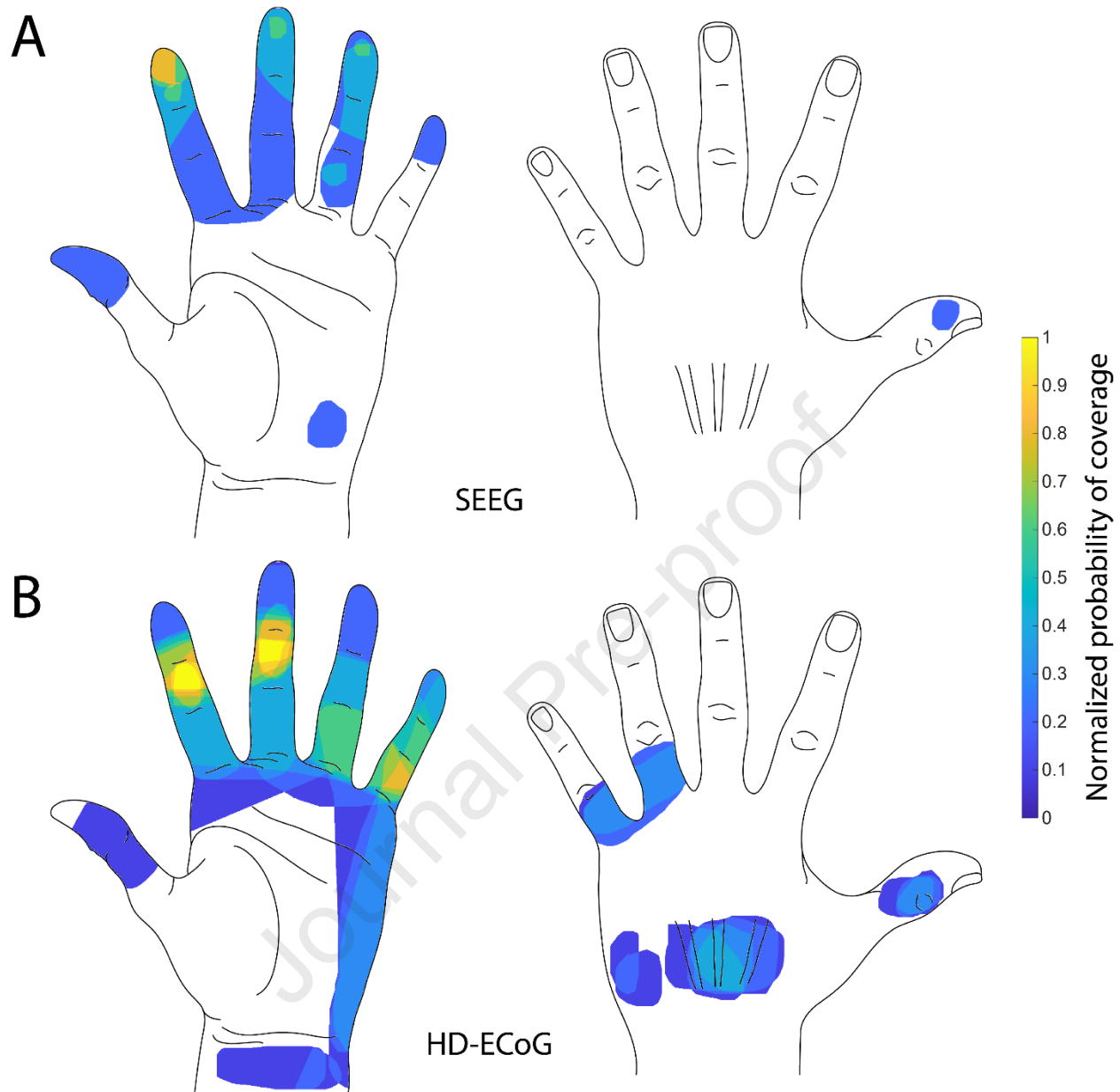
762

763 **Figure 2. Self-reported sensory percepts in the hand upon stimulation in S1 sulcal (SEEG)**  
 764 **or gyral (HD-ECoG) areas. A.** All the sensory percepts reported by participant 1 upon sulcal  
 765 stimulation through SEEG electrodes. The color of each electrode matches the color of the  
 766 corresponding percept evoked. The third panel shows a 3D brain slice showing the same SEEG  
 767 electrodes. **B.** All the sensory percepts reported by participant 1 upon gyral stimulation through  
 768 HD-ECoG electrodes. **C.** All the sensory percepts reported by participant 2 upon sulcal  
 769 stimulation through SEEG electrodes. The color of each electrode matches the color of the  
 770 corresponding percept evoked. The third panel shows a 3D brain slice showing the same SEEG  
 771 electrodes. Note the more posterior SEEG lead is not shown only in this panel but in  
 772 Supplementary Figure S3. **D.** All the sensory percepts reported by participant 2 upon gyral  
 773 stimulation through HD-ECoG electrodes. An example bipolar electrode is shown (white  
 774 rectangle). Black dashed line and white arrows denote the central sulcus.



775

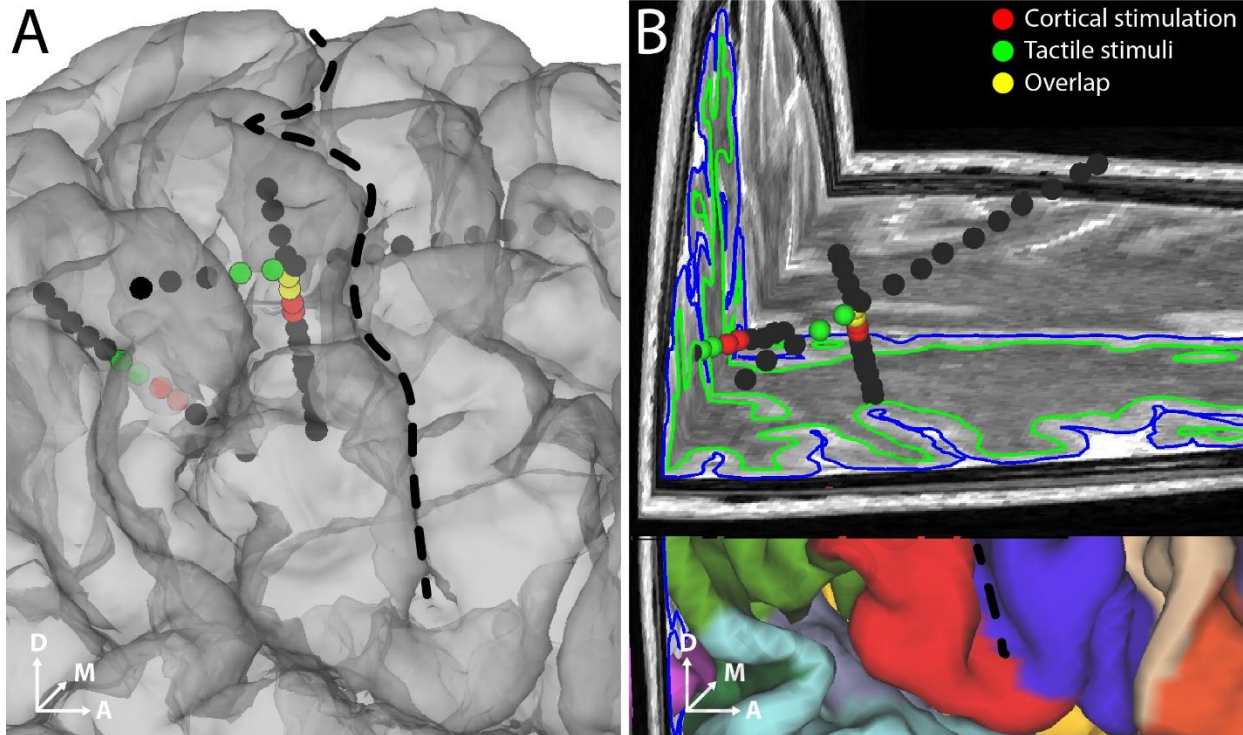
776 **Figure 3. Sensory percepts evoked by sulcal stimulation tend to be more focal in fingers. A.**  
 777 Boxplot showing the distribution of the areas covered by sensory percepts evoked by SEEG-  
 778 mediated sulcal stimulation and HD-ECoG-mediated gyral stimulation. \* denotes significance in  
 779 a Wilcoxon ranksum test,  $\chi^2 = 5.57$ ;  $p=0.02$ . **B.** Histograms showing frequency of occurrence of  
 780 percepts of different sizes for sulcal (blue) and gyral (orange) stimulation. The two distributions  
 781 are significantly different in a Kolmogorov-Smirnov test,  $p < 0.01$ .



782

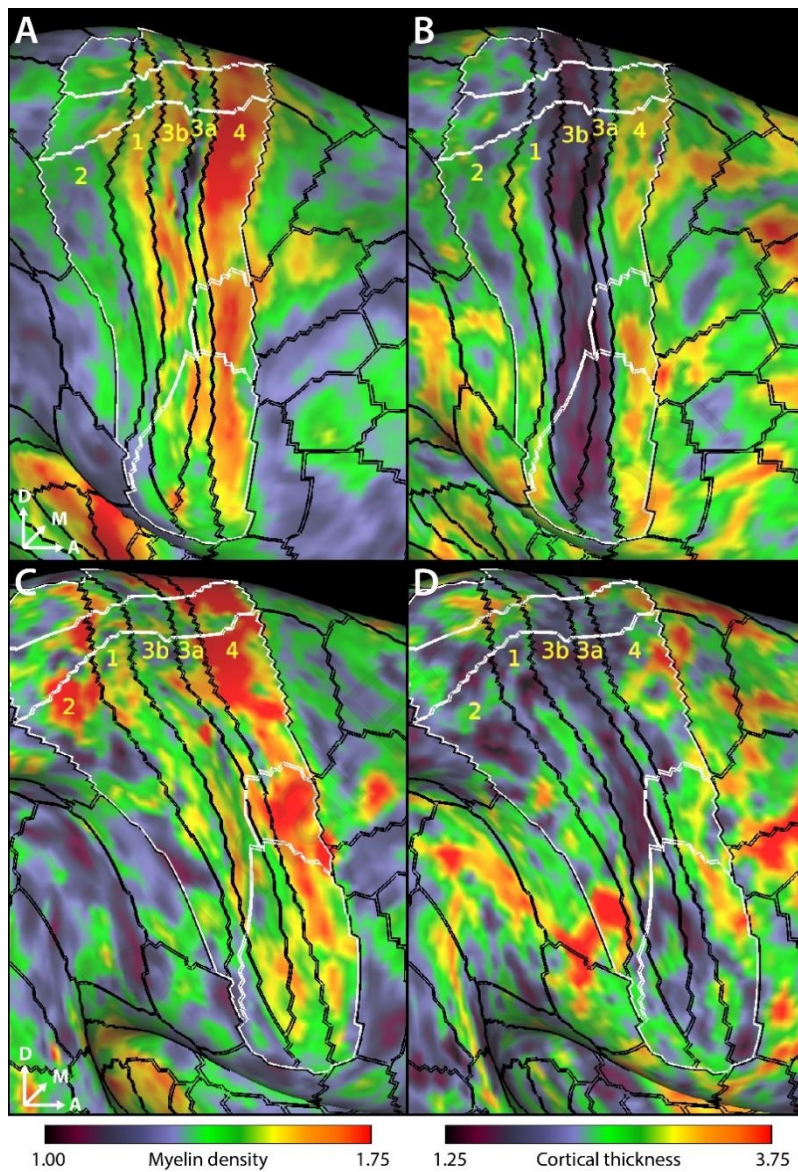
783 **Figure 4. Heatmap of evoked percepts. A.** Heatmap shows frequency of any region of the hand  
 784 being part of a sensory percept evoked by S1 sulcal stimulation pooled from both participants. **B.**  
 785 Heatmap shows frequency of any region of the hand being part of a sensory percept evoked by  
 786 S1 gyral stimulation pooled from both participants. Number of percepts covering a region of the  
 787 hand were normalized to the maximal number of percepts covering any area of the hand ( $n = 5$   
 788 for SEEG;  $n = 10$  for HD-ECoG).

789



790

791 **Figure 5. Recorded neural activity correlated with tactile stimulus of fingertips in**  
 792 **participant 2. A and B.** Electrodes that showed high degree of repeatability ( $r > 0.6$ ) of features  
 793 across mechanical tactile stimulation cycles are shown (green spheres). The electrodes that  
 794 evoked a percept in the hand area are also shown (red spheres). Overlapping electrodes are  
 795 shown in yellow. Black dashed line denotes the central sulcus. **B.** shows a 3D brain slice  
 796 showing the same SEEG electrodes.

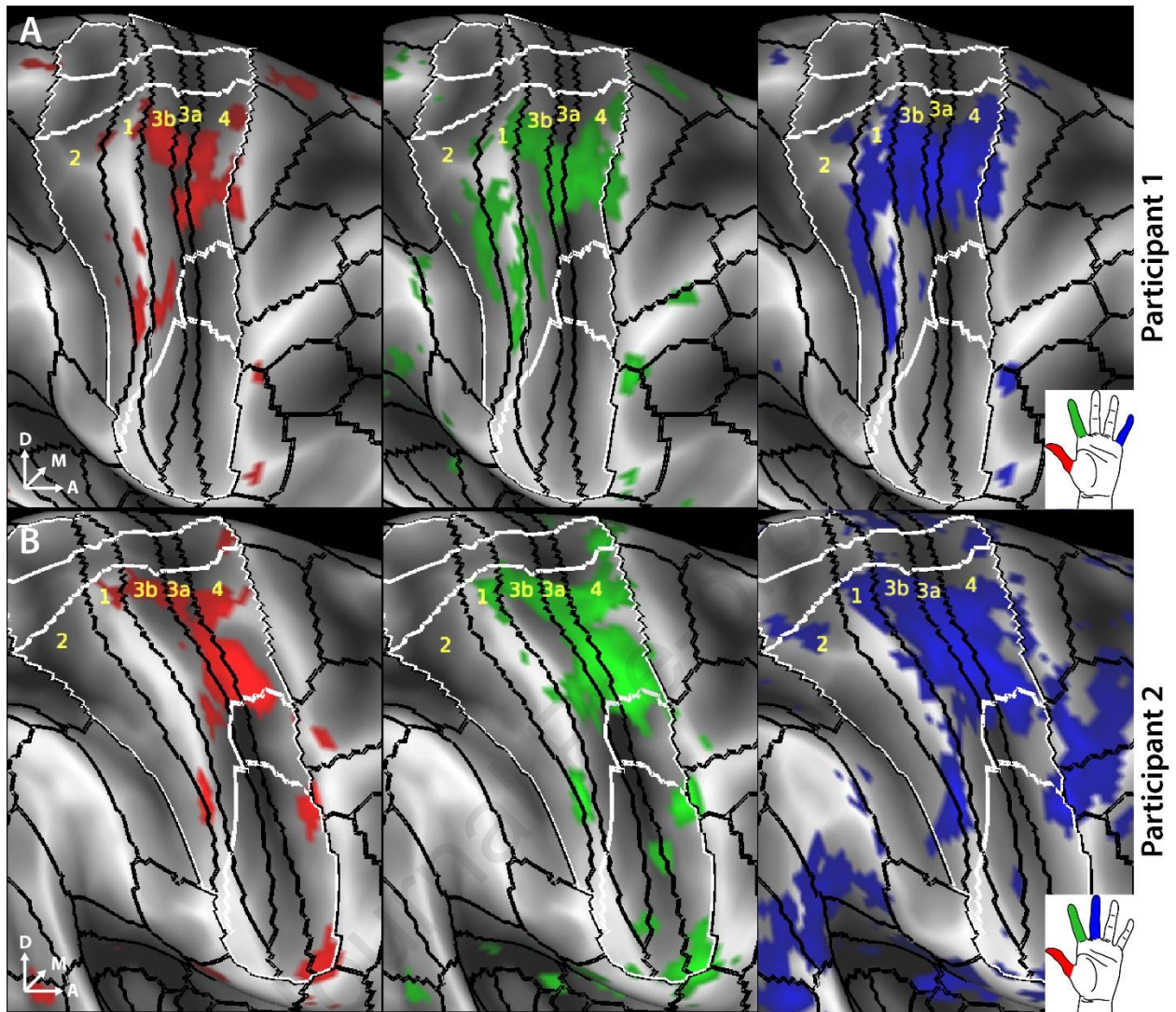
797 **Supplementary Figures**

798

799 **Fig. S1. Group cortical areal boundaries line up with individual myelin and cortical**  
 800 **thickness maps.** **A.** Color map shows the T1w/T2w-based myelin map for participant 1 as per  
 801 color bar at bottom. **B.** Color map shows the cortical thickness for participant 1 as per color bar  
 802 at bottom. **C.** Color map shows the T1w/T2w-based myelin map for participant 2. As per color  
 803 bar below. **D.** Color map shows the cortical thickness for participant 2 as per color bar below.  
 804 The black lines overlaid on the cortical surface delineate the cortical areal boundaries outside of  
 805 sensorimotor cortex and sensorimotor subregional boundaries inside sensorimotor cortex as  
 806 derived from the HCP S1200 group average parcellation [40] based on myelin and cortical

807 thickness maps and are labeled in yellow letters. The white lines demarcate the sensorimotor  
808 subregions based on resting state and task-based functional MRI. The sensorimotor subareas are  
809 denoted by the intersection of the black and white boundaries.

Journal Pre-proof

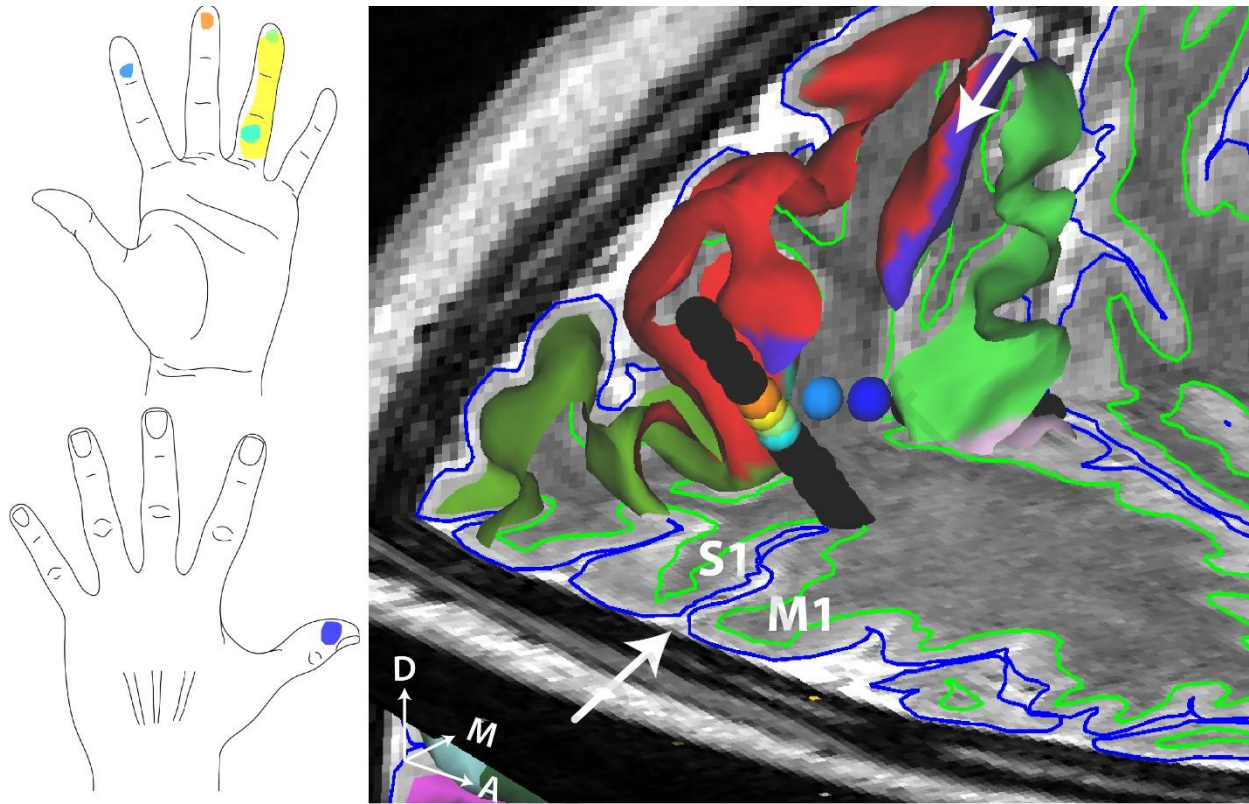


810

811 **Fig. S2. fMRI activation maps for individual digits.** Sensorimotor cortex activation map  
 812 shown in **A.** for digits D1 (red), D2 (green) and D5 (blue) in participant 1 and in **B.** for digits D1  
 813 (red), D2 (green) and D3 (blue) in participant 2 over the “very-inflated” representation of the  
 814 cortical surface (right panels). The black lines overlaid on the cortical surface delineate the  
 815 cortical areal boundaries outside of sensorimotor cortex, and sensorimotor subregional  
 816 boundaries inside sensorimotor cortex as derived from the HCP’s multimodal group average  
 817 parcellation [40] based on myelin and cortical thickness maps and are labeled in yellow letters.  
 818 The white lines demarcate the somatotopic sensorimotor subregions based on resting state and  
 819 task-based fMRI. The sensorimotor subareas are denoted by the intersection of the black and  
 820 gray shading denotes curvature of the cortical surface.

821

822



823

824 **Fig. S3. Posterior SEEG lead for participant 2.** The coronal plane lies at the postcentral sulcus  
 825 right behind the second lead (two dark blue spheres in the white matter). The color of each  
 826 electrode matches the color of the corresponding percept evoked. White arrows denote the  
 827 central sulcus. The red cortical surface denotes primary somatosensory cortex.

828

829 **Table 1. Proportion of electrode that evoked sensations.** Table showing total number of  
 830 electrodes that were observed to be in S1 and nearby white matter, number of electrodes that  
 831 evoked a sensory percept alone and number of electrodes that evoked a sensory percept in the  
 832 hand and wrist region.

<b>Participant</b>	<b>Type of electrode</b>	<b>Total in S1</b>	<b>No. of electrode pairs that evoked tactile sensation alone</b>	<b>No. of electrode pairs that evoked sensation in hand and wrist</b>
Participant 1	SEEG	28	17	5
	HD-ECOG	22	10	10
Participant 2	SEEG	28	6	6
	HD-ECOG	57	28	18

833

834 **Table 2. Sensory percept details for participant 1.** Table provides the electrode details,  
 835 stimulation parameters that evoked a sensory percept in participant 1 and the percept description.  
 836 All percepts were felt only in the contralateral (left) hand.

Electrode Type	Lead/ Grid	Electrode Pair	Threshold Amplitude (mA)	Frequency (Hz)	Percept Description
SEEG	RFp	7 – 8	0.5	20	Index and thumb
	RFp	9 – 10	0.5	20	Electrical sensation index fingertip
	RFp	10 – 11	0.8	20	Front of index and thumb
	RFp	12 – 13	3	50	Digits 1-2 and then palm
	RPa	1 – 2	0.65	20	Electrical sensation Digits 3-5, only tips
HD-ECOG	HDG	3 – 4	0.8	50	Intense tingling Digits 4-5 on dorsal surface
	HDG	4 – 5	0.72	50	Intense tingling Digits 4-5, on dorsal surface and down to the top of the palm just below
	HDG	5 – 6	0.7	50	Tingling Digits 2-5, center of digits (not fingertips), on dorsal surface
	HDG	6 – 7	1	50	Twitching sensation Digits 2-3, entire finger involved
	HDG	9 – 10	1.3	50	Tingling index finger, dorsal surface
	HDG	11 – 10	0.6	50	Tingling Digits 3-5, dorsal surface
	HDG	12 – 11	0.7	50	Tingling Digits 4-5, dorsal surface
	HDG	12 – 13	1	50	Tingling, pinky finger
	HDG	13 – 14	1.3	50	Twitching sensation in pinky
	HDG	15 – 14	1.77	50	Tingling in fingers

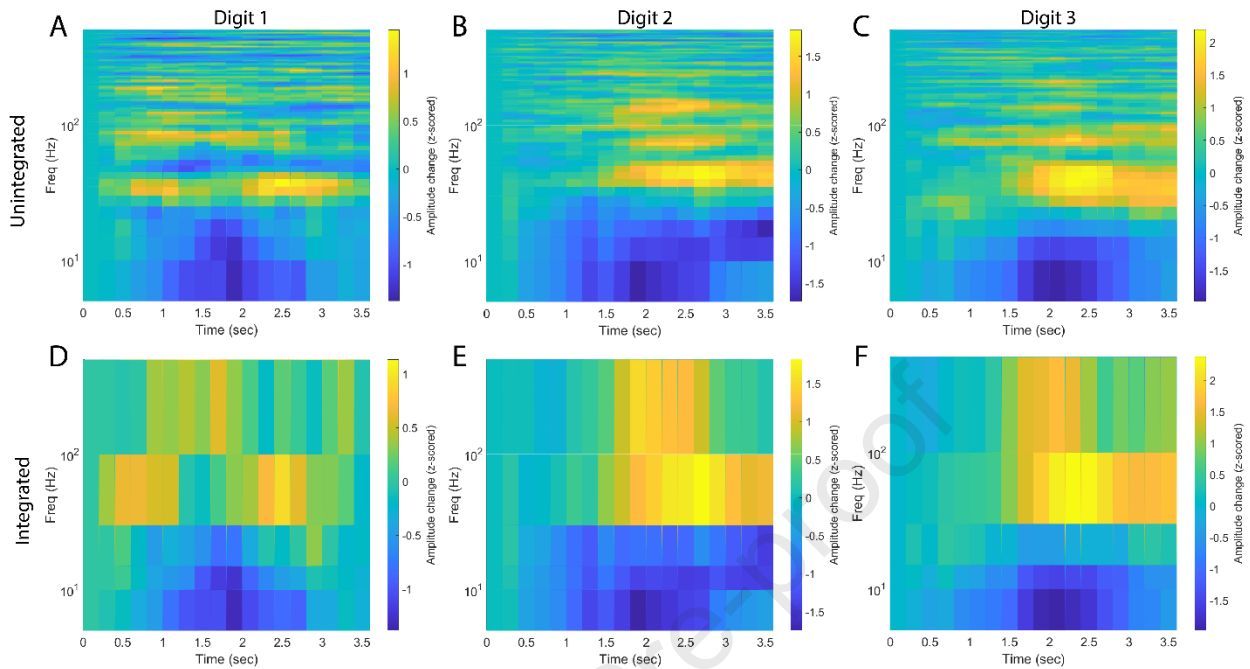
837

838

839 **Table 3. Sensory percept details for participant 2.** Table provides the electrode details,  
 840 stimulation parameters that evoked a sensory percept in participant 2 and the percept description.  
 841 All percepts were felt only in the contralateral (left) hand.

Electrode Type	Lead/ Grid	Electrode Pair	Threshold Amplitude (mA)	Frequency (Hz)	Percept Description
<b>SEEG</b>	RP <sub>s</sub>	9 – 10	0.5	20	Tingling Digit 4, towards bottom of finger
	RP <sub>s</sub>	10 – 11	0.5	20	Tingling Digit 4 fingertip; some sensation in digit 3
	RP <sub>s</sub>	11 – 12	0.65	20	Tingling, whole of digit 4
	RP <sub>s</sub>	12 – 13	1	20	Tingling, digit 3 fingertip
	RP <sub>i</sub>	5 – 6	4.8	20	Tingling by the thumb
<b>HD-ECoG</b>	RP <sub>i</sub>	6 – 7	2.1	20	Tingling index finger, small spot
	HDG	39 – 40	1.5	50	Tingling, wrist
	HDG	40 – 41	1.7	50	Tingling, wrist
	HDG	54 – 55	1.66	50	Tingling, palm
	HDG	55 – 56	1.2	50	Tingling, palm
	HDG	56 – 57	1.8	50	Tingling, palm
	HDG	57 – 58	5.7	50	Tingling, palm
	HDG	71 – 72	5.71	50	Tingling, dorsal surface below digit 5
	HDG	72 – 73	0.85	50	Tingling, dorsal surface below digit 5
	HDG	85 – 86	1.7	50	Tingling, digit 3, inside surface
	HDG	86 – 87	2.38	50	Tingling, digit 3, inside surface
	HDG	101 – 102	1.8	50	Tingling, 2 <sup>nd</sup> and 3 <sup>rd</sup> digits
	HDG	102 – 103	2.1	50	Tingling, 2 <sup>nd</sup> and 3 <sup>rd</sup> digits
	HDG	103 – 104	1.2	50	Tingling, 2 <sup>nd</sup> and 3 <sup>rd</sup> digits
	HDG	104 – 105	2.08	50	Tingling, 2 <sup>nd</sup> and 3 <sup>rd</sup> digits
HDG	116 – 117	5	50	Tingling, digit 2	
HDG	117 – 118	1.95	50	Tingling, digit 2	
HDG	147 – 148	1.95	50	Tingling, thumb (dorsal on knuckle)	
HDG	148 – 149	3.43	50	Tingling (dorsal on knuckle)	
HDG	149 – 150	2.45	50	Tingling (dorsal on knuckle)	

842



843

844 **Fig. S4. Neural responses (spectrograms) for mechanical tactile stimuli to fingertip pads. A-**845 **C.** Unintegrated spectrogram results (5 Hz resolution) averaged across all trials for tactile stimuli

846 presented to digits 1, 2, and 3, respectively. The cue period for stimuli lasted 3s and the spectral

847 response plotted represents the change in signal amplitude (z-scored) change at various

848 frequencies from the cue presentation at time=0. **D-F.** Change in integrated amplitude features

849 (integrated signal amplitudes across wider frequency ranges: 0-5, 5-10, 10-15, 15-30, 30-100,

850 and 100-500Hz, as described in the Methods section).

851

852

**Conflict / Declaration of Interest form**

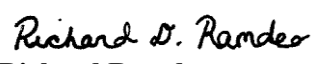
We wish to confirm that there are no known conflicts of interest associated with this publication and there has been no significant financial support for this work that could have influenced its outcome. We confirm that the manuscript has been read and approved by all named authors and that there are no other persons who satisfied the criteria for authorship but are not listed. We further confirm that the order of authors listed in the manuscript has been approved by all of us.

We confirm that we have given due consideration to the protection of intellectual property associated with this work and that there are no impediments to publication, including the timing of publication, with respect to intellectual property. In so doing we confirm that we have followed the regulations of our institutions concerning intellectual property.

We further confirm that any aspect of the work covered in this manuscript that has involved either experimental animals or human patients has been conducted with the ethical approval of all relevant bodies and that such approvals are acknowledged within the manuscript.

We understand that the Corresponding Author is the sole contact for the Editorial process (including Editorial Manager and direct communications with the office). He/she is responsible for communicating with the other authors about progress, submissions of revisions and final approval of proofs. We confirm that we have provided a current, correct email address which is accessible by the Corresponding Author and which has been configured to accept emails from the Brain Stimulation Journal

Signed by all authors as follows:

	Jan 24, 2021 Date		Jan 24, 2021 Date
<b>Santosh Chandrasekaran</b>		<b>Stephan Bickel</b>	
	Jan 25, 2021 Date		Jan 25, 2021 Date
<b>Jose L Herrero</b>		<b>Joo-won Kim</b>	
	Jan 25, 2021 Date		Jan 25, 2021 Date
<b>Noah Markowitz</b>		<b>Elizabeth Espinal</b>	
	Jan 25, 2021 Date		Jan 25, 2021 Date
<b>Nikunj A Bhagat</b>		<b>Richard Ramdeo</b>	
	Jan 25, 2021 Date		Jan 25, 2021 Date
<b>Junqian Xu</b>		<b>Matthew F Glasser</b>	
	Jan 25, 2021 Date		Jan 27, 2021 Date
<b>Chad E Bouton</b>		<b>Ashesh D Mehta</b>	